Pure & Appl. Chem., Vol. 50, pp. 1725–1762.
Pergamon Press Ltd. 1978. Printed in Great Britain.
© IUPAC
0033-4545/78/1201-1725$02.00/0

INTERNATIONAL UNION OF PURE AND APPLIED CHEMISTRY

MACROMOLECULAR DIVISION

COMMISSION ON POLYMER CHARACTERIZATION AND PROPERTIES

REPORT FROM IUPAC WORKING PARTY ON STRUCTURE AND PROPERTIES OF COMMERCIAL POLYMERS

THE EFFECT OF MOLECULAR ORIENTATION ON THE MECHANICAL PROPERTIES OF RUBBER-MODIFIED POLYSTYRENE

Prepared for publication by

W. RETTING

BASF Aktiengesellschaft, Ludwigshafen,
Federal Republic of Germany

PERGAMON PRESS
OXFORD · NEW YORK · PARIS · FRANKFURT

THE EFFECT OF MOLECULAR ORIENTATION ON THE MECHANICAL PROPERTIES OF RUBBER-MODIFIED POLYSTYRENE

A Report of the IUPAC Working Party "Structure and Properties of Commercial Polymers" being the second in a Programme of Study on Orientation in Polymers

Prepared for publication by

W. Retting

BASF Aktiengesellschaft, D-6700 Ludwigshafen, Germany

Abstract - Unoriented and oriented specimens of two rubber-modified polystyrenes (designated HIPS I and II) were examined by 8 members of the IUPAC working party "Structure and Properties of Commercial Polymers".

The raw materials were characterized by several methods. It was found that the two materials, apart from their different glass transition temperatures Tg (unlike HIPS II, HIPS I contains no paraffin oil as a lubricant), differ mainly with regard to their effective rubber phase volume: although both materials were prepared with the same rubber content, the rubber particles of HIPS II contain more polystyrene and therefore have a larger volume.

The molecular orientation of the stretched specimens, distributed to all participants, as well as of the specimens stretched individually by some participants was determined by several methods (birefringence, linear thermal expansion, frozen-in stress, shrinkage). Because of its higher Tg, HIPS I becomes more highly oriented when both materials are streched at the same temperature.

The dependence of the matrix orientation of the materials, as well as of the corresponding deformation of the embedded rubber particles, on the stretching conditions was examined. Owing to the molecular relaxation mechanisms, the orientation of the matrix relaxes during the stretching process. If the specimens are stretched with constant crosshead speed at sufficiently high temperatures, the generation and relaxation of orientation obeys the superposition principle, and in addition the generation of orientation follows a linear relationship with strain. Furthermore, if the materials are stretched within a suitable temperature range above Tg, some of their properties can be explained very well with the aid of the theory of rubber elasticity. The deformation of the rubber particles depends on the draw ratio of the matrix and on the stretching conditions. Only at low temperatures and short streching times do the rubber particles deform in conformity to the matrix. Otherwise their deformation falls short of the matrix deformation.

The influence of orientation on the mechanical properties of the materials was also investigated. Strength and extensibility, both measured parallel to the direction of orientation, are improved by orientation. The unusual increase in extensibility is due to a transition from deformation by craze formation to deformation by shear yielding. - HIPS I is somewhat stronger, especially if it is oriented, and in the oriented state is able to deform more easily by shear yielding. On the other hand HIPS II, which tends more to crazing, shows, if not oriented, an extensibility that is considerably higher than that of the unoriented HIPS I. The mechanical properties of the oriented materials are definite functions of the molecular orientation of the matrix material, independent of the stretching conditions and of the deformation of the rubber particles.

CONTENTS

1 Introduction

2 Characterization of the raw materials
2.1 General characterization of the materials
2.2 Molecular weight characterization of the polystyrene matrix
2.3 Gel content and swelling index
2.4 Glass transition temperatures
2.5 Rheological properties
2.6 Rubber particle size and size distribution

3 Preparation of the oriented specimens
3.1 Compression moulding and stretching of the specimens examined by all participants
3.2 Stretching experiments performed by individual participants

4 Molecular orientation of the polystyrene matrix
4.1 Methods used to examine the orientation
4.2 Orientation of the specimens examined by all participants
4.3 Relationships between the magnitudes used to characterize the orientation
4.4 Relaxation of the orientation during the stretching process - validity of the superposition principle
4.5 Applicability of the theory of rubber elasticity to HIPS I and II stretched at temperatures above Tg

5 Deformation of the rubber particles
5.1 Measurement of the deformation
5.2 Relationship between the deformation of the rubber particles and the macroscopic draw ratio

6 Mechanical properties of the oriented materials
6.1 Tensile properties
6.2 Impact properties
6.3 Creep properties
6.4 Time- and temperature-dependent moduli
6.5 Environmental stress cracking

7 Dependence of the mechanical properties on the orientation of the PS matrix and on the deformation of the rubber particles

8 Conclusions

1 INTRODUCTION

This paper, resulting from the work of the Working Party "Structure and Properties of Commercial Polymers" (See also (1-10)) within the Macromolecular Division of the International Union of Pure and Applied Chemistry, is one of a series concerned with the relationships between molecular orientation and mechanical properties of polymers. In the first investigation of this series (report prepared by T.T. Jones (8)) an amorphous one-phase homopolymer (polystyrene) was examined. The paper presented here gives results obtained from the examination of a more complex material, i.e. of rubber-modified polystyrene.

The participants of this study were the following:

1. ■ Central Laboratorium TNO, Delft, The Netherlands
2. ● Rhone-Poulenc, Centre de Recherches de la Croix-de-Berny, Antony, France
3. x Technical University Prague, Institute of Chemical Technology, Prague, CSSR
4. ▲ Montedison S.p.A., Research Centre of Bollate, Italy
5. □ Monsanto Chemicals Ltd., Newport, Gwent., UK
6. △ Hoechst Aktiengesellschaft, Frankfurt/Main - Hoechst, Germany
7. ◇ Cranfield Institute of Technology, Dep. of Materials, Cranfield, Bedford, UK
8. ○ BASF Aktiengesellschaft, Ludwigshafen am Rhein, Germany

Each participant will be referred to by the numbers or by the symbols shown above.

Two rubber-modified polystyrenes designated HIPS I and HIPS II were examined in this programme: one (HIPS I) was polymerized especially for this purpose, the other (HIPS II) being a commercial product. Both materials were supplied by participant 8. The programme covers the characterization of the raw materials, the examination of the orientation state of specimens stretched at temperatures near the glass transition of polystyrene up to draw ratios of 1:6, and measurements of the mechanical properties of the unoriented as well as of the oriented materials. The aim of this investigation was to find out the relationships between the characteristics of the raw material, the orientation state and the mechanical properties of rubber-modified polymers.

2 CHARACTERIZATION OF THE RAW MATERIALS

2.1 GENERAL CHARACTERIZATION OF THE MATERIALS

The materials HIPS I and HIPS II studied in this programme are rubber-modified polystyrenes with slightly differing molecular weights and molecular weight distributions (see below). The rubber content (polybutadiene) added to the polystyrene matrix was about 6 weight-percent in both cases. HIPS I, polymerized especially for this programme, was not oil-lubricated, whereas HIPS II, a commercial high-impact-polystyrene, contains about 3.5 % of paraffin oil.

The densities of HIPS I and II determined by participant 1 are 1.0384 and 1.0356 g/cm^3 respectively. No significant differences were found between the densities of the unoriented specimens and the specimens which were uniaxially stretched up to draw ratios of about 6:1.

2.2 MOLECULAR WEIGHT CHARACTERIZATION OF THE POLYSTYRENE MATRIX

The results of molecular weight measurements performed by participants 2, 3, 4, 6, and 8 are compiled in Table 1. All participants used similar methods of phase separation. The HIPS was dissolved in methyl ketone (MEK) (participants 2, 6, and 8) or in a mixture of MEK and toluene (see (11)) (participants 3 and 4). After centrifugation the insoluble part was separated as a swollen gel, poured into methanol and dried in order to determine the gel content and the swelling indices of the materials (see 2.3). The dissolved part of HIPS was precipitated by methanol and, after having been dissolved once more in suitable solvents, used for GPC and viscosity measurements. Participant 4 also carried out the phase separation by successive dissolution in MEK and toluene.

As shown in Table 1 there are some discrepancies between the molecular weight data of several laboratories which may be due to a different calibration of the GPC columns and also to differences in separating the polystyrene from the rubber phase (see 2.3). Nevertheless it can be concluded that the characteristics of the molecular weight of the two samples do not differ very much: $\bar{M}_n$ of HIPS II is slightly lower than $\bar{M}_n$ of HIPS I, whereas $\bar{M}_w$ of both samples is nearly equal. Consequently the polydispersity of HIPS II is slightly higher than that of HIPS I.

2.3 GEL CONTENT AND SWELLING INDEX

The weight fraction of the gel phase was determined by participants 2, 3, 4, and 8. Furthermore participant 4 also measured the content of polybutadiene in the gel. The results of these measurements are summarized in Table 2. As one can see in every case HIPS I has lower values of gel content but higher values of swelling index. Differences between the participants' results are presumably due to differences in the washing procedure, to a different swelling of the centrifugated gel, and also to a different drying of the gel (12).

The content of rubber is lower in the gel phase of HIPS II than in the gel phase of HIPS I. It must be concluded from this finding that the rubber particles of HIPS II contain a higher content of polystyrene than those of HIPS I (see also 2.4 and 2.6).

TABLE 1

Molecular weight and molecular weight distribution

Sample	Participant	$\bar{M}_n$, GPC	$\bar{M}_n$, OS	$\bar{M}_w$, GPC	$\bar{M}_w$, LS	$\bar{M}_w/\bar{M}_n$	M_v	Remarks
HIPS I	2	112 000	—	204 000	—	1.8	202 000	Laboratory A: 2 measurements
		112 000	—	219 000	—	2.0	205 000	([η] in tetrahydrofuran)
	2	94 400	—	202 000	—	2.1	—	Laboratory B
	2	98 500	—	199 500	—	2.0	—	Spherosil,axial diff.corrected
	2	103 000	—	214 000	—	2.1	—	Waters, Styragel diff.corrected
	3	—	—	—	—	—	234 000	[η] measured in toluene
	4	72 000	112 000	201 000	—	2.8(1.8)	185 000	"
	6	106 000	—	206 000	—	1.9	183 000	"
	8	70 000	—	182 000	210 000	2.6(3.0)	222 000	"
HIPS II	2	82 000	—	192 000	—	2.3	197 500	Laboratory A: 2 measurements
		96 000	—	219 000	—	2.3	—	([η] in tetrahydrofuran)
	2	78 600	—	195 200	—	2.5	—	Laboratory B
	2	81 500	—	182 000	—	2.2	—	Spherosil,axial diff.corrected
	2	88 000	—	205 000	—	2.3	—	Waters,Styragel diff.corrected
	3	—	—	—	—	—	149 000	[η] measured in toluene
	4	63 000	88 000	189 000	—	3.0(2.1)	182 000	"
	6	94 000	—	198 000	—	2.1	170 000	"
	8	58 000	—	178 000	196 000	3.1(3.4)	217 000	"

$\bar{M}_n$ = number average molecular weight — GPC = gel-permeation-chromatography

$\bar{M}_w$ = weight average molecular weight — OS = osmometry

$\bar{M}_v$ = viscosity molecular weight — LS = light scattering

$[\eta]$ = intrinsic viscosity [l/g]

$[\eta] = K \cdot \bar{M}_v^a$ [l/g]; $a = 0.725$; $K = \begin{cases} 1.17 \text{ l/g} & \text{for tetrahydrofuran} \\ 1.10 \text{ l/g} & \text{for toluene} \end{cases}$

TABLE 2

Gel content and swelling index

Sample	Participant	Number of extractions	Gel content (%)	Content of PB in the Gel (%)	Swelling index SI	Remarks
HIPS I	2	1	19.2		11.1	
		3	10.7		4.6	
	3	1	15.7		15.5	
	4	1	15.0	38.0	16.1	SI: toluene only
		1	14.6			MEK, toluene successively
	8	1	18.1		11.5	
HIPS II	2	1	25.9		10.7	
		3	17.0		3.6	
	3	1	20.0		14.4	
	4	1	20.9	27.0	14.2	SI: toluene only
		1	19.2			MEK, toluene successively
	8	1	25.0		11.5	

TABLE 3

Glass transition temperatures of the matrix and the rubbery phase

Sample	Participant	Method	Frequency (Hz)	Tg(PS) (°C)	Tg(Rubber) (°C)	Remarks
HIPS I	1	TP	1	113	- 90	const.frequency
	1	BV	100	—	- 78	
	1	BV	1000	—	- 72	
	2	DSC	—	102	—	
	4	TP	1	—	90	
	4	DSC	—	101	—	
	6	TP	1	—	- 89	
	6	DSC	—	100	- 95	
	8	TP	1	110	- 87	const.frequency
HIPS II	1	TP	1	—	- 85	const.frequency
	1	BV	100	—	- 74	
	1	BV	1000	—	- 68	
	2	DSC	—	92	—	
	4	TP	1	—	- 85	
	4	DSC	—	92	—	
	6	TP	1	—	- 85	
	6	DSC	—	91	- 93	
	8	TP	1	106	- 86	const.frequency

TP = torsion pendulum

BV = bending vibration

DSC = differential scanning calorimeter

2.4 GLASS TRANSITION TEMPERATURES

The glass transition temperatures Tg of the polystyrene matrix and the rubbery phase, measured by participants 1, 2, 4, 6 and 8, are presented in Table 3. In addition, Fig. 1 shows the mean loss factor and the modulus curves of HIPS I and II based on torsion pendulum measurements of participants 1, 4, 6, and 8. Corresponding to the apparently higher rubber content of HIPS II (see 2.3) the rubber peak of HIPS II is higher and broader than that of HIPS I.

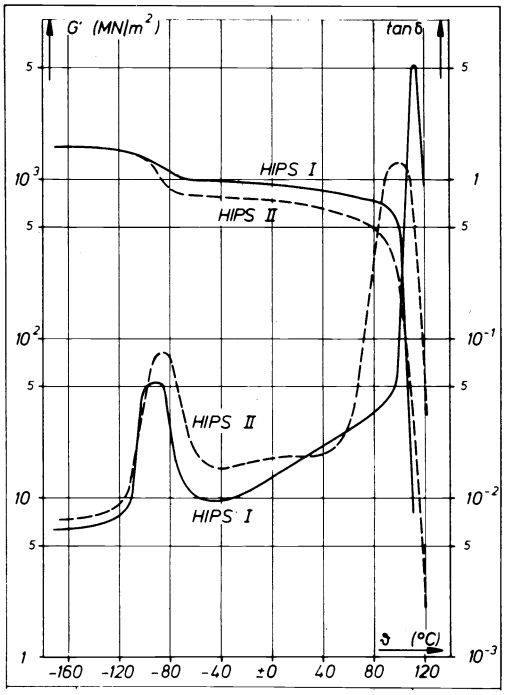

Fig. 1. Average shear modulus (G') and loss factor (tan δ) curves of HIPS I and II taken from torsion pendulum measurements of participants 1, 4, 6, and 8. (Frequency 1 Hz).

From Table 1 as well as from Fig. 1 it can be gathered that the glass transition temperature of the polystyrene matrix of HIPS I is distinctly higher than that of HIPS II, owing to the absence of oil lubricant in the first-mentioned material.

Participant 1 also carried out torsion pendulum measurements on oriented specimens (draw ratio 6:1). He found that orientation slightly lowers the rubber peak, but that its temperature location remains unaffected. At temperatures above the rubber peak the orientation reduces the damping but increases the moduli.

2.5 RHEOLOGICAL PROPERTIES

The melt viscosities of HIPS I and II were determined by participants 2 and 4 with the aid respectively of Instron and Goettfert capillary rheometer devices. Participant 2 applied the Bagley and the Rabinowitch corrections to his measuring results whereas participant 4 did not apply any correction. The results of these measurements are shown in Figs. 2 and 3. As is to be seen, the oil content of HIPS II obviously decreases the viscosity of this material.

Participant 2 also found that the die swell (ratio of extrudate diameter to capillary diameter) of both materials is a linear function of the shear stress at the wall (Fig. 4), independent of the temperature and only slightly dependent on the L/D ratio (L/D between 4 and 40). This linear relationship was observed even beyond the shear stress at which melt fracture occurs (between 0.14 and 0.16 MN/m^2).

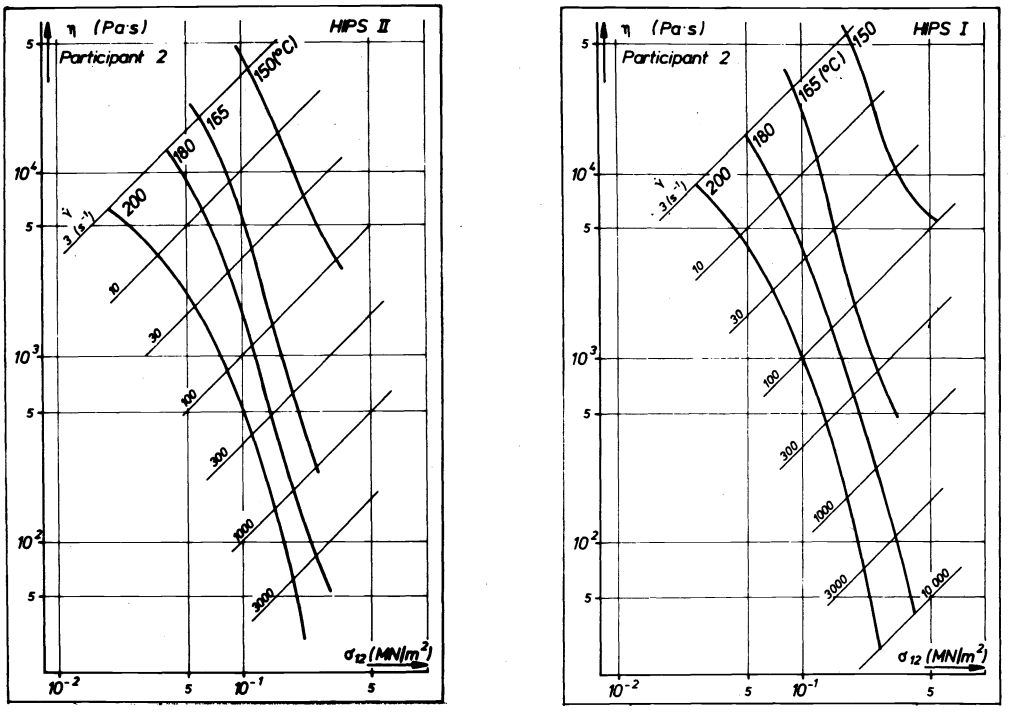

Fig. 2. Melt viscosity η as a function of the shear stress σ_{12}, parameters strain rate and temperature. a) HIPS I b) HIPS II

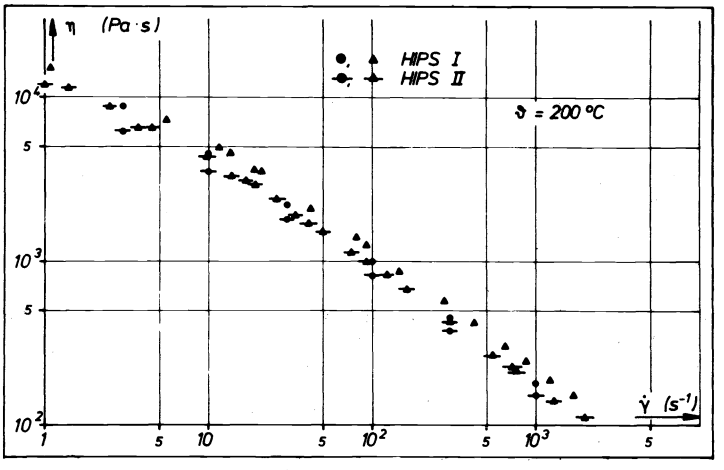

Fig. 3. Flow curves of HIPS I and II (melt viscosity η as a function of the strain rate $\dot{\gamma}$), temperature 200 °C.

2.6 RUBBER PARTICLE SIZE AND SIZE DISTRIBUTION

Participants 2, 4, and 8 measured the rubber particle size by means of optical microscopy (part. 2 and 4) and of electron microscopy (part. 2 and 8). As an example Fig. 5 shows electron micrographs of the two materials. Also this Fig. indicates that the rubber particles of HIPS II contain more polystyrene than the particles of HIPS I.
The evaluation of all the micrographs in accordance with a procedure reported by Cigna (11) and, in addition, with the aid of a method described by Gerrens (13) led to the following results: the two materials differ only a little with regard to their particle size and scarcely at all with regard to the size distribution. But HIPS I seems to contain a larger number of deformed and disturbed particles. The mean particle diameter

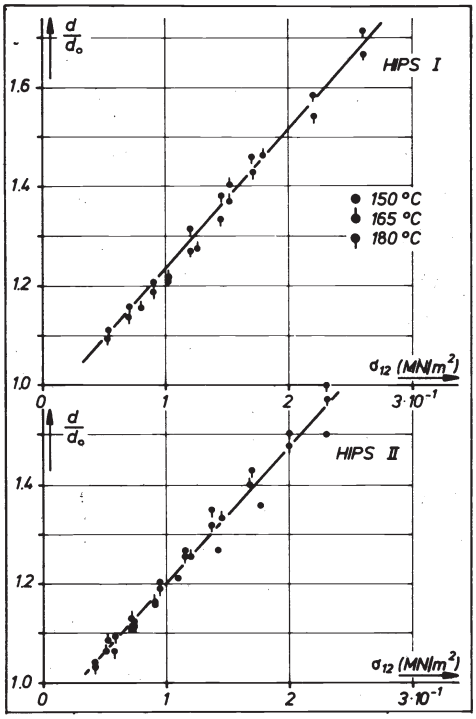

Fig. 4. Die swell d/d_0 of HIPS I and II as a function of the shear stress σ_{12}.

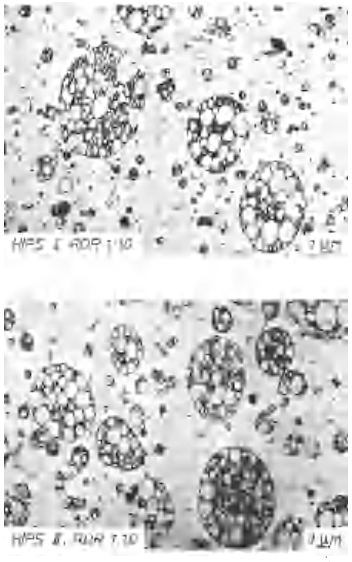

is about 3 μm (part. 4) whereas the most frequent diameter is about 8 μm (part. 2). The mass distribution of the particle size shows a flat maximum between 4 and 5 μm for HIPS I and between 6 and 7 μm for HIPS II; and in both cases a range from less than 1 μm to more than 10 μm (part. 8).

3 PREPARATION OF THE ORIENTED SPECIMENS

3.1 COMPRESSION MOULDING AND STRETCHING OF THE SPECIMENS EXAMINED BY ALL PARTICIPANTS

From HIPS I and II raw materials participant 8 firstly prepared plaques of different thicknesses by compression moulding in order to obtain sheets of nearly equal thickness (1 mm) after stretching to different draw ratios. The temperature of the press plates was about 180 °C.

Before being stretched, all plaques were marked with a 2 x 2 cm square pattern in order to render possible a subsequent determination of the real draw ratio of each specimen taken from those plaques. The stretching of the moulded plaques to nominal draw ratios (NDR) of 1:2.5, 1:4.5, and 1:6 was carried out with the aid of a biaxial stretching machine manufactured by the Breitner Comp. at Siegdorf/Germany. The plaques were clamped only in the direction of the drawing. The clamps could run freely in the transverse direction. Therefore at least the middle part of the sheets was drawn nearly uniaxially without greatly hindering the transverse contraction.

Only this middle part was used to perform experiments on the oriented materials. The stretching temperature was 130 °C. Since the stretching time should be the same for all specimens, namely 15 s, the stretching speed had to be varied in accordance with the draw ratio and the plate geometry. Fig. 6 gives a survey on the geometrical conditions of the stretching procedure.

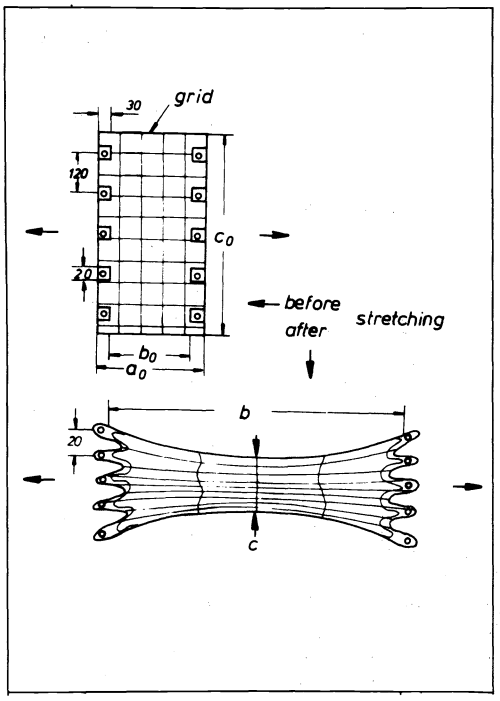

Fig. 6. Geometrical conditions of plaque stretching
NDR = nominal draw ratio, dimensions in mm.

NDR	a	b_0	→	b	c_0	→	c
2.5	500	440		1100	500		400
4.5	300	240		1200	500		250
6.0	200	140		980	600		250

Only the approximately uniaxially stretched middle parts of the plaques were used to perform all experiments.

3.2 STRETCHING EXPERIMENTS PERFORMED BY INDIVIDUAL PARTICIPANTS

Stretching experiments were carried out by participants 2 and 8 in order to examine the dependence of the molecular orientation and of the properties of the oriented materials on the stretching conditions.

Participant 2 subjected unoriented specimens (which he himself had prepared from the raw materials) to uniaxial as well as to biaxial extension in the temperature range between Tg + 10 °C and Tg + 30 °C. The strain rate $\dot{\varepsilon}$ was held constant during stretching by a special device which is described in (14): $\dot{\varepsilon}$ was 0.15 s^{-1} for uniaxial stretching, and 0.05 s^{-1} for biaxial stretching. For uniaxial stretching rectangular specimens of 40 x 5 x 1 mm were used. To perform the biaxial extension experiments participant 2 inflated circular specimens (radius 75 mm, thickness 1 mm) with the aid of N_2 pressure. Stress and strain values were calculated from the continuously recorded pressure, the bubble height, and the lateral distance between two points in the polar region of the bubble (see (14)).

Participant 8 performed uniaxial stretching experiments on rectangular strips (width 18 to 20 mm) which were cut from the unoriented sheets (thickness 1 mm) delivered to all the participants in this programme. Not the strain rate but the stretching speed was kept constant in these experiments. Furthermore, by contrast with participant 2, participant 8 did not use the strain rate but the stretching time as a variable in addition to the stretching temperature and the draw ratio. The reason for doing so was to compare specimens which had the same chance to decrease their molecular orientation by relaxation processes. Furthermore the specimens stretched by participant 8 were considerably thicker than those stretched by participant 2.

The stretching time t_{str}, the stretching temperature ϑ_{str}, and the draw ratio DR were varied by participant 8 in the range between

t_{str} : 30 s and 3000 s

ϑ_{str} : 100 °C (HIPS II) or 105 °C (HIPS I) and 130 °C

DR : 1:1 and about 1:6

In addition to the stretching experiments participant 8 also carried out some annealing experiments at constant draw ratio on oriented specimens in order to find out whether a definite relationship exists between the molecular orientation and the mechanical properties (see also (7), (8) and section 7 of this report).

4 MOLECULAR ORIENTATION OF THE POLYSTYRENE MATRIX

4.1 METHODS USED TO EXAMINE THE ORIENTATION

To determine the orientation state of the materials under test the following methods were applied:

4.1.1 Birefringence measurements were carried out by participant 6 on the oriented specimens, distributed to all the participants in this programme, as well as on the specimens stretched individually by participant 8. Participant 6 used an optical microscope under conditions of conoscopic observation. The instrument was equipped with a Berek compensator and a Bertrand lens. He was able to examine the original bulk specimens up to an optical retardation of 70 orders. Since a simple estimation showed that the form birefringence due to the elliptical shape of the rubber particles can be neglected in this case the birefringence determined in the way described is a sufficiently good messure of the molecular orientation of the materials under test.

4.1.2 The coefficient α of linear thermal expansion (LTE) was evaluated as a measure of orientation by participants 1 and 8. As for all quantities which can be described by a second rank tensor, the following relationship holds good for the LTE coefficient of an uniaxially oriented material (see e.g. (15)):

$$(\alpha_\perp - \alpha_\parallel)/(\alpha_2 - \alpha_1) = (3\,\overline{\cos^2\vartheta} - 1)/2 \qquad (1)$$

where $\alpha_\parallel$ ($\alpha_\perp$) is the observed LTE parallel (perpendicular) to the stretching direction and α_1 (α_2) the LTE of the perfectly oriented material parallel (perpendicular) to the chain axis; ϑ is the angle between the principal axis of a statistical molecular segment and the stretching direction. The right hand term of equation (1) is identical with Hermans' orientation function (16)

$$f_{or} = \Delta n/\Delta n_{max} = (3\,\overline{\cos^2\vartheta} - 1)/2 \qquad (2)$$

where Δn and Δn_{max} are respectively the birefringence of the partially and the perfectly oriented material.

Furthermore (see (17)) the α_1 value of a polymeric material should be nearly equal to the thermal expansion coefficient of low molecular weight materials with merely covalent bonds. Such is the case with quartz glass for which α is about 5.10^{-7} K^{-1}. This value is very low compared with the thermal expansion coefficient α_o of an isotropic polymer material ($\alpha_o \approx 10^{-5}$ to 10^{-4} K^{-1}). Furthermore α_2 is higher than α_o. Consequently α_1 can be neglected with respect to α_2, in the present case. In consideration of this fact, there follows from equation (1) and the trivial relationship

$$\alpha_{\parallel} + 2\alpha_{\perp} = 3\alpha_o = \alpha_1 + 2\alpha_2 \qquad (3)$$

the equation

$$(\alpha_{\perp} - \alpha_{\parallel})/(\alpha_2 - \alpha_1) = f_{or} \approx (\alpha_{\perp} - \alpha_{\parallel})/\alpha_2 = 1 - \alpha_{\parallel}/\alpha_o \ . \qquad (4)$$

This equation, which by contrast with equation (2) allows the determination not only of the relative but also of the absolute orientation function, contains only a minor error that is due to the neglect of α_1. This error is at most about 1 % because at complete orientation $\alpha_{\parallel}$ is equal to α_1 and consequently $f_{or} \approx 0.99$ instead of the correct value of one.

Of course, the "orientation function" of the whole two-phase HIPS system is measured in this way. But fortunately the difference between the thermal expansion coefficients α_R and α_{PS} of the rubber particles and the polystyrene matrix respectively, which is considerable at low strains, disappears when the material is stretched up to a certain range. This behaviour is due to the well-known fact that the thermal expansion coefficient of rubbers decreases very steeply with increasing draw ratio and finally becomes negative (conversely the temperature of rubber specimens rises if they are stretched sufficiently - negative thermomechanical effect). Thus, at draw ratios of the rubber particles between 2 and 5 (which values correspond to axial ratios of about 3 and 10 and to the draw ratios 2 and 4 of the matrix - see 5.2 and Fig. 22) the influence of α_R on the expansion coefficient α of the whole system can be neglected to a fairly good approximation. This can be gathered from Fig. 7 where, as an example, some α values of HIPS I are plotted with DR as abscissa and the stretching temperature as parameter, the stretching time being 30 s for all specimens. As is to be seen, the α curves measured at higher draw ratios can be extrapolated to a point α_o on the ordinate axis the position of which is independent of the stretching temperature (and also of the stretching time). Furthermore α_o is identical for HIPS I and II and, in addition, nearly equal to α values determined on specimens of unoriented pure polystyrene. For instance, on samples of the polystyrenes A and B, which were examined during a former programme of the working party (see (8)), α was subsequently determined and found to be $7.5\ 10^{-5}$ and $7.3\ 10^{-5}$ K^{-1} respectively. When taking the points on the α curves, which lead to α_o, as the $\alpha_{\parallel}$ values, and α_o as the expansion coefficient of the unoriented matrix material, the orientation function f_{or} of the matrix can be determined with the aid of equation (4) to a good approximation. This, in addition, is confirmed by the proportionality of f_{or} measured in this way and Δn, a relationship which was found to be valid for all specimens (see 4.3).

4.1.3 The frozen-in stress of the oriented specimens was determined by participants 1, 2, 3, 4, 6, and 8, who all carried out shrinkage force measurements. Although the conditions of these measurements performed by the individual laboratories varied over a rather wide range (free length of the clamped specimens between 50 and 175 mm, rate of temperature increase between 2 and 6 °C/min) the scatter of the results was not too great (see section 4.2). This is due to the fact that a variation of the heating rate up to at least 4 °C/min does not influence the results remarkably (participant 1).

Participant 2 performed experiments on specimens prepared and oriented by himself (see section 2.2) in order to separate the entropic stress part σ_E of the frozen-in stress from the energy-elastic part (see also (10) and (8)). This is possible because at temperatures close to Tg the relaxation of the energy-elastic stress is faster than that of the entropic stress.

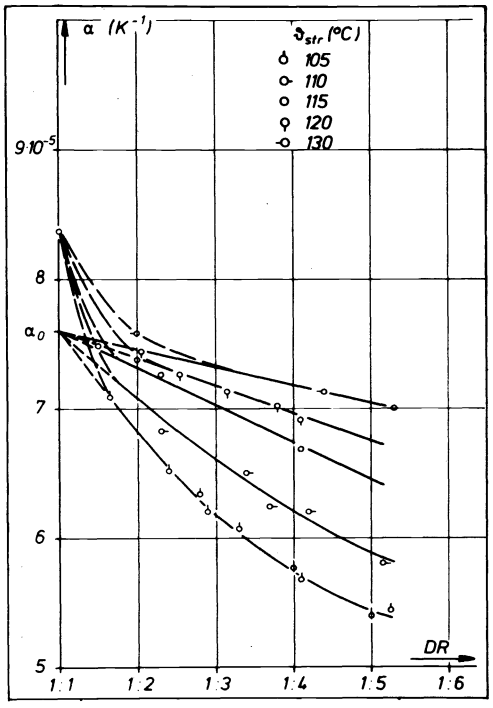

Fig. 7. Temperature coefficient α of linear thermal expansion measured on HIPS I specimens in the temperature range between 10 and 40 °C. Specimens stretched at constant but different stretching speeds, the stretching time being 30 s for all the draw ratios DR. Parameter: stretching temperature. α_0 = extrapolated α value of the unoriented matrix material.

Two methods of stress separation were applied by participant 2. The first consists in an isothermal relaxation experiment on oriented samples rapidly heated to a temperature a few degrees above Tg (Fig. 8a). The second and more accurate method is based on a combined shrinkage - shrinkage force experiment (Fig. 8b). Indeed, if an oriented sample is allowed to shrink a small amount, the associated decrease of internal stress will be due mainly to the relaxation of the energy-elastic stress. Consequently it may be assumed that after a sufficient amount of shrinkage the residual stress is essentially of entropic nature.

Provided that during the stretching process at temperatures just above Tg the polymer molecules behave like a Gaussian network or, in other words, that the theory of ideal rubber elasticity is at least approximately applicable to polymers having non-permanent entanglements if they are stretched in their quasi rubber-elastic temperature range, the following relationship should hold (18):

$$\sigma_E = G_\infty \, (\lambda^2 - 1/\lambda), \tag{5}$$

where G_∞ is the equilibrium shear modulus and λ = DR is the draw ratio, and furthermore

$$\Delta n/\sigma_E = (2\pi/45\ kT)\ \ ((\bar{n}^2 + 2)^2/\bar{n})\ \ (a_1 - a_2) = \text{const}, \tag{6}$$

where Δn is the birefringence of the oriented material, $\bar{n}$ is the mean refractive index, and a_1 and a_2 are the principal polarizabilities of the statistical molecule segment (see also (8)). Equations (5) and (6) render it possible to check the validity of the theory of rubber elasticity in the present case.

4.1.4 Shrinkage measurements were carried out by participants 1, 4, and 8. Participant 1 used specimens about 50 mm long and 15 mm wide, cut with the length parallel or perpendicular to the drawing direction. After the dimensions of the specimens had been measured they were placed on a layer of talcum powder and transferred to an oven showing the desired temperature (90 - 130 °C). One hour later the specimens were removed from the oven and cooled rapidly.

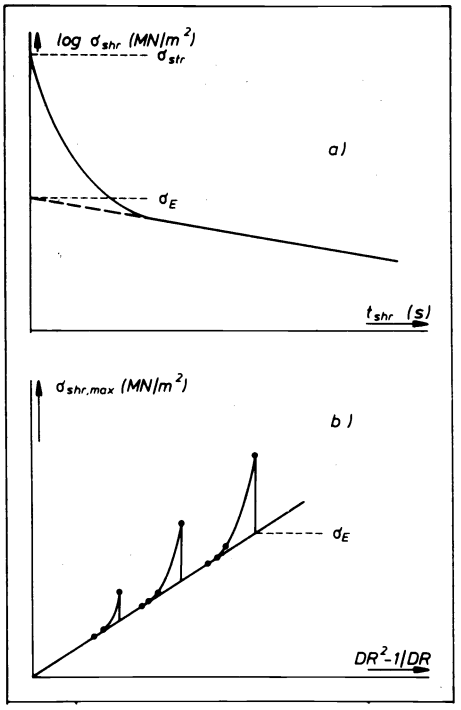

Fig. 8. Methods used by participant 2 to separate the entropic stress part σ_E from the energy-elastic part of the frozen-in stress of oriented polymers (demonstrated schematically); $\sigma_{shr,max}$ resp. σ_{shr} = (maximal) shrinkage stress, t_{shr} = shrinkage time, DR = draw ratio.

The specimens used by participant 4 were 30 mm long and 20 mm wide; the length was always parallel to the drawing direction. Participant 4 shrank the specimens for 10 to 20 min in a thermostat bath (140 °C ± 0.02 °C) filled with polyethylene-oxide of low molecular weight.

Participant 8 also applied a shrinkage temperature of 140 °C to the specimens (length about 20 mm and width about 5 mm) but used air as environmental medium and found that at this temperature heating longer than 5 minutes does not yield a higher shrinkage than obtained within this period.

As an example Fig. 9 shows the results of some shrinkage measurements of participant 1. Obviously the length reversion ratio l_1/l_2 of all specimens is nearly equal to their draw ratio, i.e. the elongation of the drawn specimens is almost reversible. Furthermore it can be gathered from Fig. 9 that the width expansion ratio b_2/b_1 falls increasingly short of the square root of l_1/l_2, the higher the draw ratio. Participant 1 also measured the thickness of all specimens and found their volume to remain constant during the shrinkage process. It follows from this result that the width expansion is different from the thickness expansion. In all probability these findings are due to the part which the biaxial orientation plays in the specimens distributed to all participants (see Fig. 6) and which cannot be neglected completely.

4.2 ORIENTATION OF THE SPECIMENS EXAMINED BY ALL PARTICIPANTS

Figs. 10 to 13 show the optical birefringence Δn (measured by participant 6), the orientation function $f_{or} = (3\ \overline{\cos^2\vartheta} - 1)/2$, which was calculated from the linear thermal expansion coefficient α (see 4.1.2) (measured by participants 1 and 8), the maximal shrinkage stress $\sigma_{shr,max}$ (measured by participants 1, 3, 4, 6, and 8), and the length reversion ratio LRR (shrinkage) (measured by participants 1, 4, and 8) of the unoriented and the oriented specimens of HIPS I and II which had been distributed to all the participants. Δn, f_{or}, $\sigma_{shr,max}$, and LRR are plotted as functions of the draw ratio DR taken from the grid which was printed on the compression-moulded plaques before stretching.

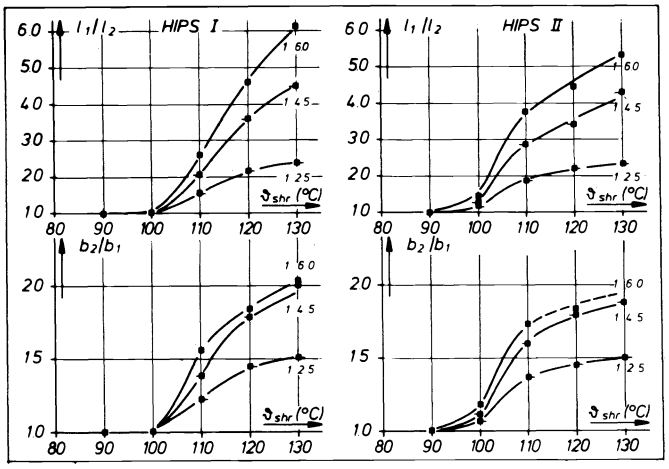

Fig. 9. Shrinkage measurements of participant 1 on the oriented sheets distributed to all participants. Specimens cut parallel to the drawing direction.

l_1, b_1, l_2 and b_2 are respectively length and width of the specimens before and after shrinkage.

ϑ_{shr} = shrinkage temperature, the shrinkage time was 1 h.

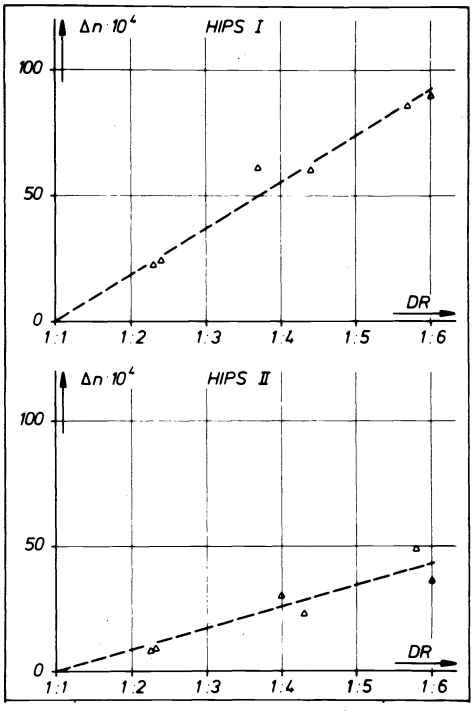

Fig. 10. Birefringence Δn of HIPS I and II (distributed sheets) as a function of the draw ratio DR.

As is to be seen Δn, f_{or} and LRR are all linear functions of DR, which is due to the fact that all of the specimens were stretched at the same temperature (130 °C) and, in spite of different draw ratios, within the same stretching time (15 sec) (see 4.4). Only $\sigma_{shr,max}$, at least at higher draw ratios, seems not to be a linear function of DR.

Although the scatter in Δn as a function of DR (or vice versa) is rather great and, in addition, there is seen to be a systematic deviation of the α values measured by participant 8 from those measured by participant 1, there can be no doubt that the orientation of HIPS I exceeds that of HIPS II

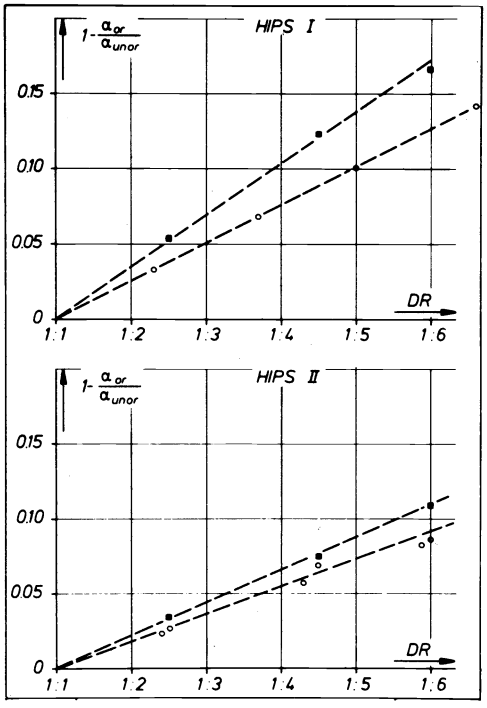

Fig. 11. Orientation function $f_{or} \approx 1 - (\alpha_{or}/\alpha_{unor})$ of HIPS I and II (distributed sheets) as a function of the draw ratio DR. α_{or} and α_{unor} = temperature coefficients of linear thermal expansion of the unoriented and of the oriented materials respectively (measured by two participants).

considerably. This is due of course to the fact that the glass transition temperature Tg of HIPS I is higher than that of HIPS II and, therefore, the orientation of HIPS II is able to decrease more easily by relaxation during the stretching process (see also 4.4).

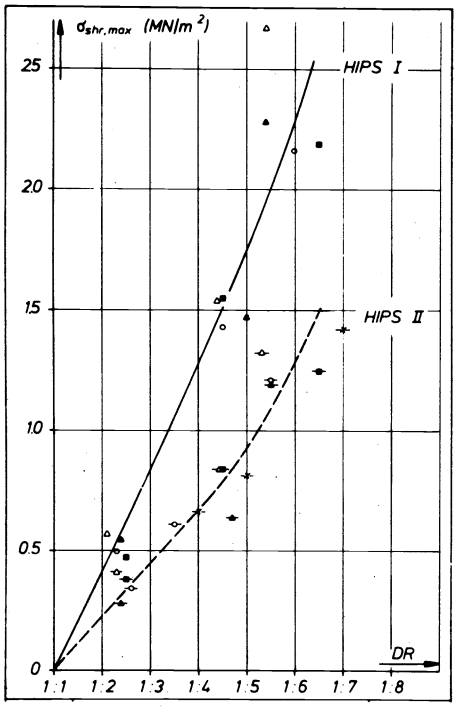

Fig. 12. Maximal shrinkage stress $\sigma_{shr,max}$ of HIPS I and II (distributed sheets) as a function of the draw ratio DR

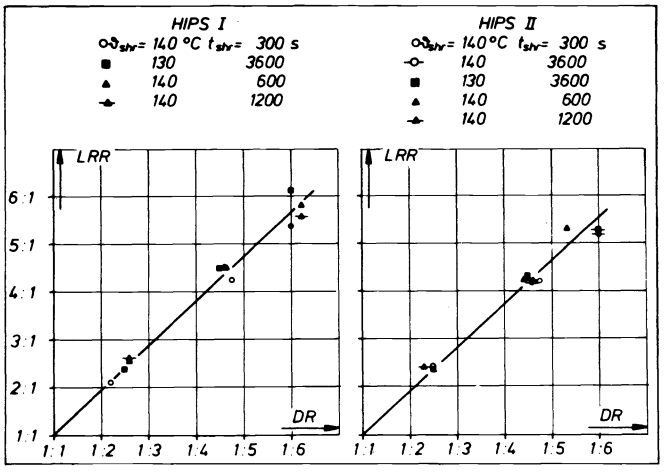

Fig. 13. Length reversion ratio LRR of HIPS I and II (distributed sheets) as a function of the draw ratio DR

ϑ_{shr} = shrinkage temperature, t_{shr} = shrinkage time, shrinkage measured parallel to the drawing direction.

4.3 RELATIONSHIP BETWEEN THE MAGNITUDES USED TO CHARACTERIZE THE ORIENTATION

Figs. 14 to 16 show the results of measurements which were carried out by participants 2, 6, and 8 on specimens of HIPS I (and partly of HIPS II, too) individually stretched by participant 8 under various conditions, i.e. at various stretching temperatures and with constant but different stretching speeds. The speeds were chosen in such a way that series of specimens with different draw ratios but equal stretching temperatures and equal stretching times could be compared, These measurements were undertaken in order to find out the relationships between the magnitudes used to characterize the orientation state of the specimens and their dependence on the stretching conditions.

In Fig. 14 the orientation, calculated from the linear thermal expansion coefficient α of the HIPS I and II specimens, is plotted against their birefringence Δn. As is to be seen, for both materials the relation between $1 - (\alpha_{or}/\alpha_{unor})$ and Δn appears to be independent of the temperature and the stretching time and is given by a straight line the slope of which, however, is different for HIPS I and HIPS II. There are at least two possible reasons for this difference: 1) The optical anisotropy of the molecules may be modified by the paraffin oil in HIPS II, 2) the form effect, due to the rubber particles, may be different on account of the different polystyrene content in the effective rubber phase.

In Fig. 15 the maximal shrinkage stress σ_{shr} and its entropic part σ_E (measured by participant 2, see 4.1.3) of the HIPS I specimens are shown as functions of Δn. The stretching time of these specimens was 30 sec and the stretching temperatures were 105 and 120 °C. Neither σ_{str} nor σ_E are linear functions of Δn. However, if Δn does not exceed values of about $100 \cdot 10^{-4}$ these functions can be approximated by linear relationships.

Finally Fig. 16 shows the shrinkage (length reversion ratio LRR) of HIPS I specimens drawn at various temperatures ϑ_{str} within various times t_{str} as a function of Δn. The shrinkage temperature ϑ_{shr} and the shrinkage time t_{shr} were 140 °C and 5 minutes. For each series of measurements with constant ϑ_{str} and t_{str} but varied draw ratio DR the LRR values are situated on definite but nonlinear curves. The draw ratio seems to be completely reversible in any case, with the exception of the specimens drawn at 130 °C within 30 sec. At this high temperature and within this relatively long time obviously a small amount of real, i.e. irreversible flow occured.

Summarizing the results of the measurements reported in this section, one can state the following: of all the magnitudes used to measure the orientation of the specimens stretched by participant 8, only $f_{or} = 1 - \alpha_{or}/\alpha_{unor}$ and Δn turned out to be proportional one to the other. Furthermore the relationship between f_{or} and Δn is independent of the stretching temperature and the stretching time (but not of the material

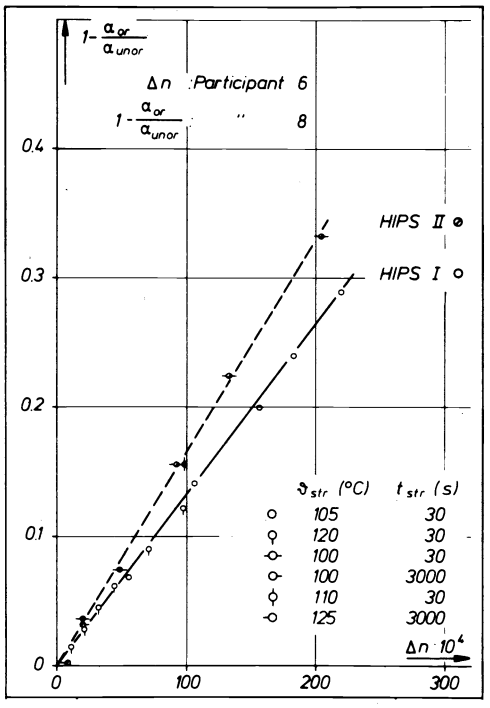

Fig. 14. Orientation function calculated from the linear thermal expansion coefficient α of specimens of HIPS I and II streched under various conditions but with constant speed as a function of their birefringence Δn.

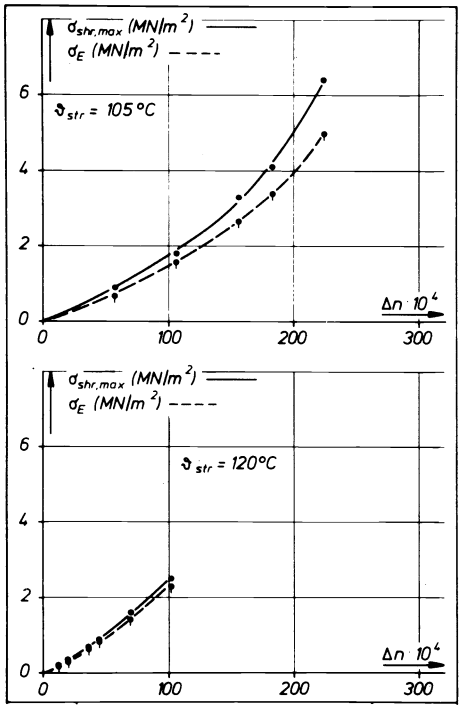

Fig. 15. Maximal shrinkage stress $\sigma_{shr,max}$ and its entropic part σ_E of specimens of HIPS I stretched with constant speed at 105 and 120 °C within 30 sec as functions of their birefringence Δn.

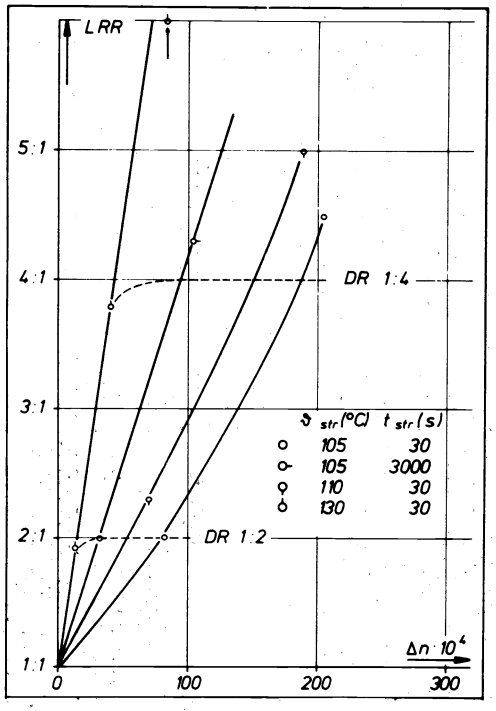

Fig. 16. Length reversion ratio LRR obtained from shrinkage experiments on specimens of HIPS I stretched under various conditions but with constant speed as a function of their birefringence Δn. Shrinkage temperature ϑ_{shr} = 140 °C, shrinkage time t_{shr} = 5 minutes.

----- = points of equal draw ratio (1 : 4 partly interpolated)

under test). Consequently these quantities seem to be the best possible for characterizing the orientation of the materials examined here.

4.4 RELAXATION OF THE ORIENTATION DURING THE STRETCHING PROCESS - VALIDITY OF THE SUPERPOSITION PRINCIPLE

Fig. 17 shows the orientation functions (calculated from the linear thermal expansion) of specimens of HIPS I and II, which were stretched by participant 8 under various conditions but with constant speed, as function of the stretching temperature ϑ_{str}, the stretching time t_{str} being used as a parameter. The draw ratio of all these specimens was 1:2. As is to be seen, at constant draw ratio DR the orientation decreases with increasing stretching temperature and increasing stretching time, which findings are due to the fact that the molecular relaxation mechanisms cause a relative decrease of the orientation during the stretching process (7, 19).

This relaxation of the orientation can be compared with the stress relaxation of a viscoelastic material subjected to a tensile test at room temperature within the range of linear viscoelasticity. This range, which at room temperature is limited to elongations of a few tenths of one percent, is characterized by the validity of the superposition principle (see (20) e.g.).

It is now possible to check whether the superposition principle also holds good for the orientation of certain viscoelastic materials which are stretched at temperatures above Tg up to the much higher extensions of some hundred percent. If such is the case it must be possible to describe the orientation by the formula (see (20))

$$f_{or}(\varepsilon,t) \sim \Delta n(\varepsilon,t) \sim \int_0^t (d\, g\,[\varepsilon(\xi)]/d\xi)\, f\,(t-\xi)\, d\xi$$

$$= \int_0^t (d\, g(\varepsilon)/d\varepsilon)\,(d\varepsilon/d\xi)\, f\,(t-\xi)\, d\xi \qquad (7)$$

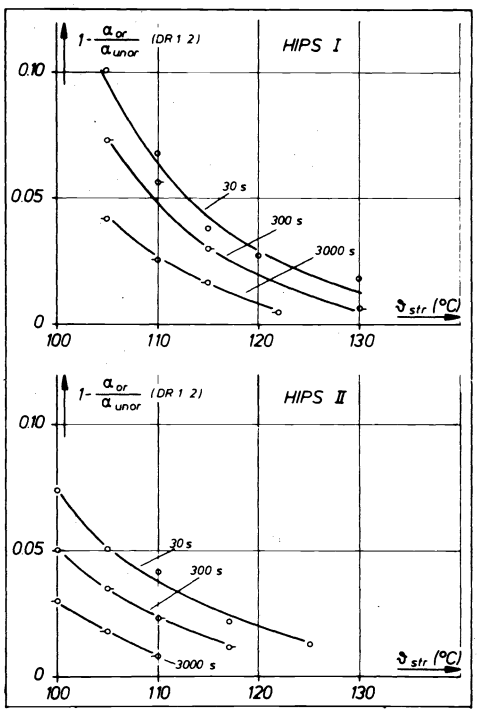

Fig. 17. Orientation function calculated from the linear thermal expansion coefficient α of specimens of HIPS I and II stretched under various conditions but with constant speed as a function of the stretching temperature ϑ_{str}.

Parameter: stretching time t_{str}.

where ε = DR−1; DR = draw ratio
t = stretching time
g = strain-dependent part of the orientation
f = time-dependent part of the orientation.

If the specimen, having the initial length l_o, is drawn with constant crosshead speed v_o then

$$\varepsilon = (v_o/l_o) \cdot t$$

and eq. (7) becomes

$$\Delta n(\varepsilon,t)/\varepsilon \sim t^{-1} \int_0^t (d\, g(\varepsilon)/d\varepsilon)\, f\,(t - \xi)\, d\xi \qquad (8)$$

In this equation the quotient $\Delta n/\varepsilon$ would depend only on the time and not on the strain if g is a linear function of ε. In this case - and only in this case - Δn, measured on specimens stretched at a given temperature up to various draw ratios but within the same stretching time, should be a linear function of ε. As is to be seen from Fig. 18 (see also Figs. 10 and 11) this linear relationship will be found if the stretching temperature is sufficiently high and the stretching time is not too short. At ϑ_{str} = 105 °C and t_{str} = 30 s the linearity is no longer observed. This, in addition, was the only case where the stress-strain curves showed a pronounced yield point.

In all the other cases the superposition principle (with the additional condition that the orientation is a linear function of the strain) can be applied to the dependence of the orientation on the strain history. (For details see (21)). As a consequence, the same orientation is obtained in these cases, e.g., if the specimen in question is stretched to a certain DR with a constant stretching speed during the time t_{str} or if the stretching experiment is performed up to the same DR but with a higher speed, i.e. within a shorter time, and the specimen is then held at constant elongation until finally t_{str} is reached. This fact was utilized by

participant 8, who diminished the orientation of given specimens by annealing them at constant DR (see section 7).

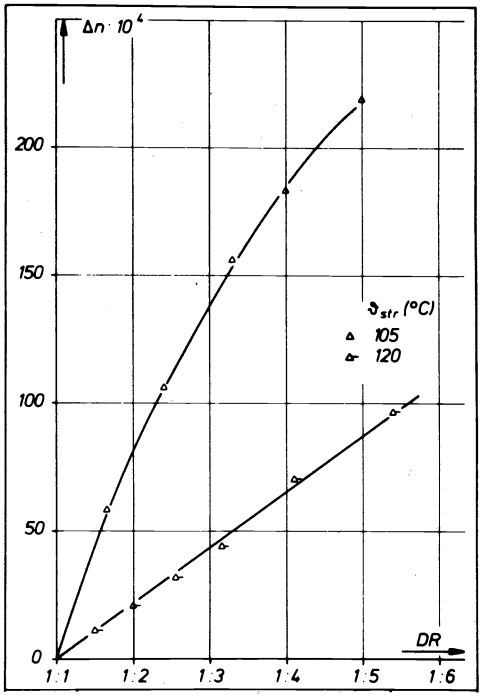

Fig. 18. Birefringence Δn of specimens of HIPS I stretched at 105 and 120 °C within 30 sec as a function of the draw ratio DR.

4.5 APPLICABILITY OF THE THEORY OF RUBBER ELASTICITY TO HIPS I AND II STRETCHED AT TEMPERATURES ABOVE TG

In Fig. 19 and 20 the results of the stretching experiments are to be seen, which participant 2 individually performed on self-prepared specimens. These specimens were considerably thinner than those distributed to all the participants and also thinner than the specimens stretched by participant 8 (see 3.2 and 4.3). Furthermore participant 2 carried out the stretching experiments with a true constant strain rate $\dot{\varepsilon} = 0.15\ s^{-1}$ (see 3.2).

From Fig. 20 it follows that the theory of rubber elasticity may be applied very well to the entropic part σ_E of the frozen-in stress (see 4.1.3, eq. (5)). In addition, the same could be concluded from the biaxial stretching experiments of participant 2 (see 3.2).

Later on, participant 2 also applied the methods for separating the entropic part σ_E from the energy elastic part of the frozen-in stress to the specimens individually stretched by participant 8 (see 3.2 and 4.3).

In this case, σ_E was found to be related linearly to $DR^2 - 1/DR$ only in the region up to $DR^2 - 1/DR \approx 10$ for $\vartheta_{str} = 105\ ^\circ C$, or up to $DR^2 - 1/DR \approx 20$ for $\vartheta_{str} = 120\ ^\circ C$. Furthermore, the σ_E values of these specimens could be approximated by a linear function of the birefringence Δn (up to $\Delta n \approx 100\ 10^{-4}$) (see 4.1.3 eq. (6)) only for $\vartheta_{str} = 120\ ^\circ C$. For $\vartheta_{str} = 105\ ^\circ C$ no linearity of this relation was found at all.

It may therefore be concluded that the applicability of the theory of the rubber elasticity to the materials under test is restricted to specimens stretched at temperatures sufficiently high above Tg but, of course, not exceeding Tg so much that easy slippage of the chain molecules prevents their treatment as a Gaussian network. In addition, the thickness of the specimens, the homogeneity of their orientation as well as differences of the stretching mode (constant speed - constant strain rate) may also cause some differences in the stretching behaviour.

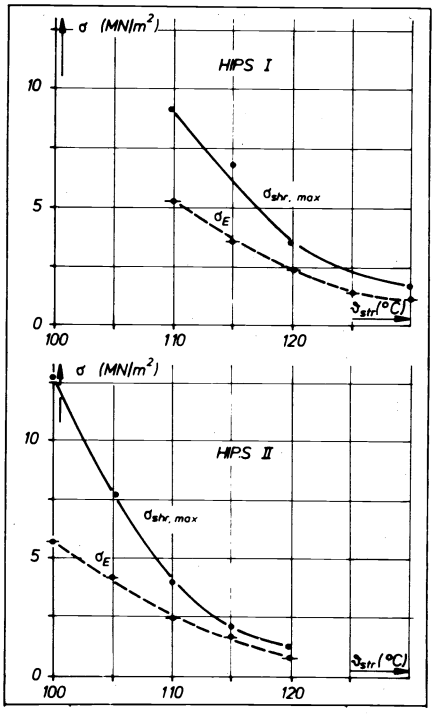

Fig. 19. Maximal shrinkage stress $\sigma_{shr\ max}$ and its entropic part σ_E of specimens of HIPS I and II stretched with true constant strain rate $\dot{\varepsilon} = 0.15\ s^{-1}$ as a function of the stretching temperature ϑ_{str}.

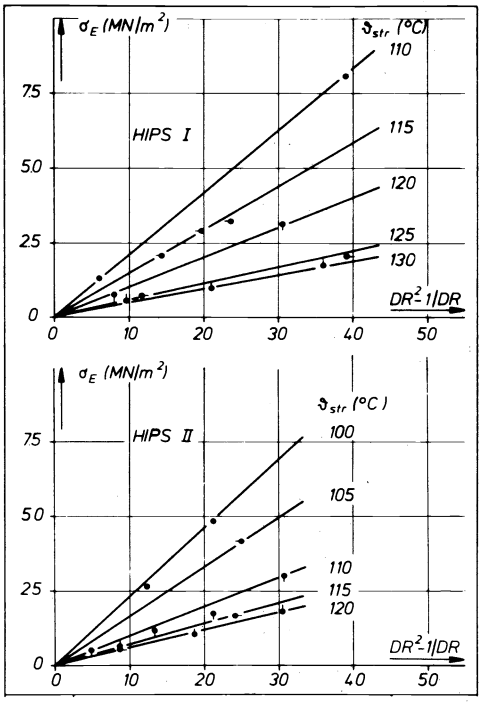

Fig. 20. Entropic part σ_E of the maximal shrinkage stress of specimens of HIPS I and II stretched with true constant strain rate $\dot{\varepsilon} = 0.15\ s^{-1}$ as a function of $DR^2 - 1/DR$ (DR = draw ratio); parameter: stretching temperature ϑ_{str}.

5 DEFORMATION OF THE RUBBER PARTICLES

5.1 MEASUREMENT OF THE DEFORMATION

The effect of uniaxial extension of the HIPS materials on the deformation of the rubber particles was studied by participant 4 by means of optical microscopy and by participants 2 and 8 using electron microscopy. Participants 4 and 8 examined the specimens distributed to all participants and participant 8 also studied the specimens stretched by himself individually under various conditions (see 3.2). All the specimens mentioned were drawn with a constant drawing speed. Participant 2 determined the deformation of the rubber particles of specimens prepared and drawn by himself at temperatures equal to Tg + 18 °C (120 °C for HIPS I and 110 °C for HIPS II) up to a draw ratio of 1:5. These stretching experiments were carried out with a true constant strain rate of 0.15 s^{-1} (see 3.2). Participant 4 made micrographs in phase contrast of sections about 2 µm in thickness. The sections were cut at room temperature parallel to xy, xz, and yz planes (x-axis parallel to the drawing direction, y-axis parallel to the width of the sheet, z-axis perpendicular to the plane of the sheet). The mean length $\overline{L}$ of the rubber particles was measured on xz sections; the mean diameter $\overline{\emptyset} = 1.33\ \overline{c}$ (where $\overline{c}$ is the mean chord (22)) was determined on yz sections. From these data the axial ratio $R = \overline{L}/\overline{\emptyset}$ of the rubber particles was calculated.

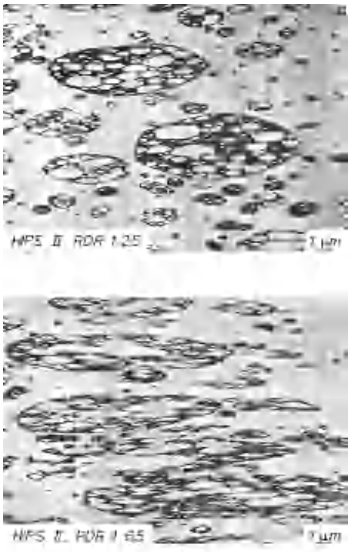

Fig. 21. Electron micrographs of the rubber particles in oriented specimens of HIPS II. RDR = real draw ratio, taken from the grid printed on the specimens before stretching.

Participants 2 and 8 determined R directly from the electron micrographs taken from microtome cuts parallel to the drawing direction (an example is shown in Fig. 21). When evaluating the micrographs the distortion of the particles in the cutting direction was taken into consideration (see also Fig. 5).

5.2 RELATIONSHIP BETWEEN THE DEFORMATION OF THE RUBBER PARTICLES AND THE MACROSCOPIC DRAW RATIO

Fig. 22 shows the results of participants 4 and 8. If the deformation of the rubber particles followed completely the draw ratio DR of the PS matrix, the axial ratio R ought to be equal to $(DR)^{3/2}$. As the figure indicates, R reaches this theoretical value to a lesser degree, the higher the DR and the higher the chosen stretching temperature or the longer the stretching time. Only at the extremely low temperature of 105 °C (HIPS I) or 100 °C (HIPS II) do the rubber particles show a deformation which conforms to that of the matrix material. Because of the different stretching mode the results of participant 2 are not considered in Fig. 22. But, in principle, these

measurements confirm the results shown in the figure: Participant 2 found for both materials an axial ratio of about 6 instead of the theoretical value $5^{3/2} = 11.18$.

The reason of this finding must be the competition between the external deformation force and the internal retractive force, caused by the elasticity of the rubber particles, acting against one another in the boundary region of the two phases. At the end of the stretching process this competition normally leads to axial ratios of the rubber particles which fall short of the theoretical R values. Of course, the final deformation of the rubber particles does not represent an equilibrium value but rather a frozen-in state which depends on the stretching time (or rate), the temperature, the draw ratio and also on the rate of cooling the specimens after stretching.

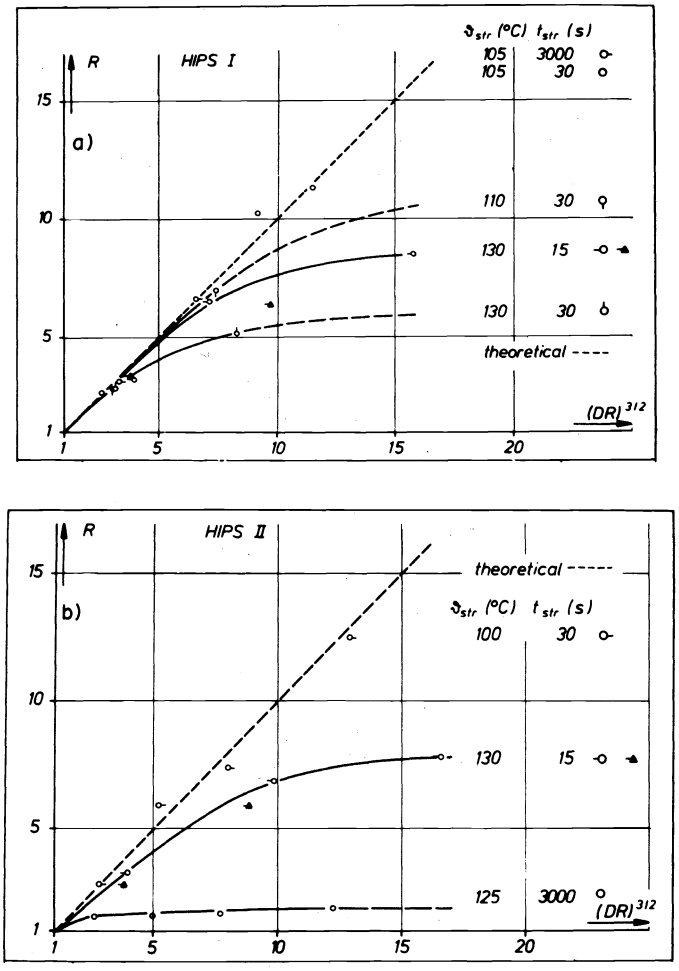

Fig. 22. Mean axial ratio R of the rubber particles in oriented specimens of HIPS I (a) and II (b) as a function of $(DR)^{3/2}$ (DR = draw ratio). The specimens were drawn with constant stretching speed under various conditions.

6 MECHANICAL PROPERTIES OF THE ORIENTED MATERIALS

6.1 TENSILE PROPERTIES

Participants 3, 6, and 8 carried out tensile tests on oriented as well as on unoriented specimens of both materials at several tensile speeds and temperatures and at different angles with respect to the drawing direction of the sheets. All these participants used specimens according to ISO R 527, type 1. Furthermore participant 1 contributed some results measured on unoriented specimens at temperatures around and above Tg. He used smaller specimens (according to DIN 53 448). The specimens were machined and polished by some participants. Conventional tensile testing machines and,

in addition, a hydraulic high-speed testing apparatus were used for the tests.

The results of these measurements are shown in Figs. 23 to 27. For both materials the yield stress σ_y and the rupture stress σ_R increase with increasing strain rate, decreasing temperature, and increasing (parallel test) or decreasing (perpendicular test) draw ratio. Both σ_y and σ_R show higher values for HIPS I than for HIPS II. This latter finding reflects the lower rubber phase volume of HIPS I (see 2.3). The different tensile behaviour of the unoriented specimens at elevated temperatures (Fig. 27) can be explained by the different Tg values.

The extensibilities of the materials are strongly influenced by their ability to deform by crazing and/or shear yielding, depending on the draw ratio, the strain rate, the temperature, and the tensile direction with respect to the direction of the orientation. At lower draw ratios the extension is mainly due to craze formation whereas at higher draw ratios shear yielding is the predominant deformation mechanism. Although this is true for both materials there are distinct differences between the tensile behaviour of HIPS I and II. From Figs. 23 to 27 as well as from Fig. 28, where for a fixed speed the tensile data of the two materials are directly compared with each other as functions of their orientation; and, in addition, from the stress-strain curves and the appearence of the tested specimens the following can be concluded:

HIPS II tends to form crazes more readily than HIPS I, which fact may be due to the higher rubber phase volume of the first-mentioned material. Therefore, when comparing the unoriented materials with each other, one finds that the extensibility of HIPS II is considerably higher than that of HIPS I (see Fig. 28 e.g.). On the other hand, if the materials are oriented, the extensibility of HIPS I exceeds that of HIPS II, at least in the range of medium orientation. This is due to the fact that the shear yielding which is the determining strain mechanism in this case is stopped prematurely by local thermal softening in the HIPS II specimens (see (9)e.g.) whereas this is not the case in the HIPS I specimens. Possibly, the higher rubber phase volume and/or thereby the higher craze volume of HIPS II is responsible for this different behaviour.
At certain strain rates both materials, if sufficiently drawn, show relatively steep decreases of the rupture strain ε_R with increasing strain rate. In the case of HIPS I this step is due to a transition from deformation by shear yielding to deformation by crazing. Therefore the step is shifted here towards higher strain rates when the draw ratio increases. By contrast, the step is caused in HIPS II by the transition between a certain degree of deformation by shear yielding and the mentioned premature rupture by thermal softening of the material. Consequently the position of this step remains nearly constant as the draw ratio increases. As is to be expected increasing temperature causes similar effects to decreasing strain rate (see Figs. 25 and 26).

6.2 IMPACT PROPERTIES

The Izod impact resistance of the unoriented sheets of both materials, supplied by participant 8, was determined by participant 2. He measured a value 75 kJ/m^2 for HIPS I and a value 76 kJ/m^2 for HIPS II.

Participant 8 carried aut Charpy impact tests (according to DIN 53 453) on the unoriented as well as on the oriented specimens, with the main axis of the specimens directed parallel and perpendicular to the drawing direction. In the first case notched specimens were used, whereas in the second case the tests were performed with unnotched specimens. The results of these measurements are shown in Fig. 29. As is to be seen the impact resistance of the unoriented specimens, measured parallel to the drawing direction, is equal for both materials, but for specimens oriented up to a certain degree the resistance of HIPS I exceeds that of HIPS II considerably. Measured perpendicular to the drawing direction, the impact resistance of the oriented as well as of the unoriented specimens of HIPS I is somewhat higher than that of HIPS II.

Multiaxial penetration tests on unoriented and on oriented specimens of HIPS I and II were performed by participants 4 and 8. Participant 4 used an apparatus developed by Montedison (23) whereas participant 8 carried out the tests according to DIN 53 443 (see also (24)). But since the testing

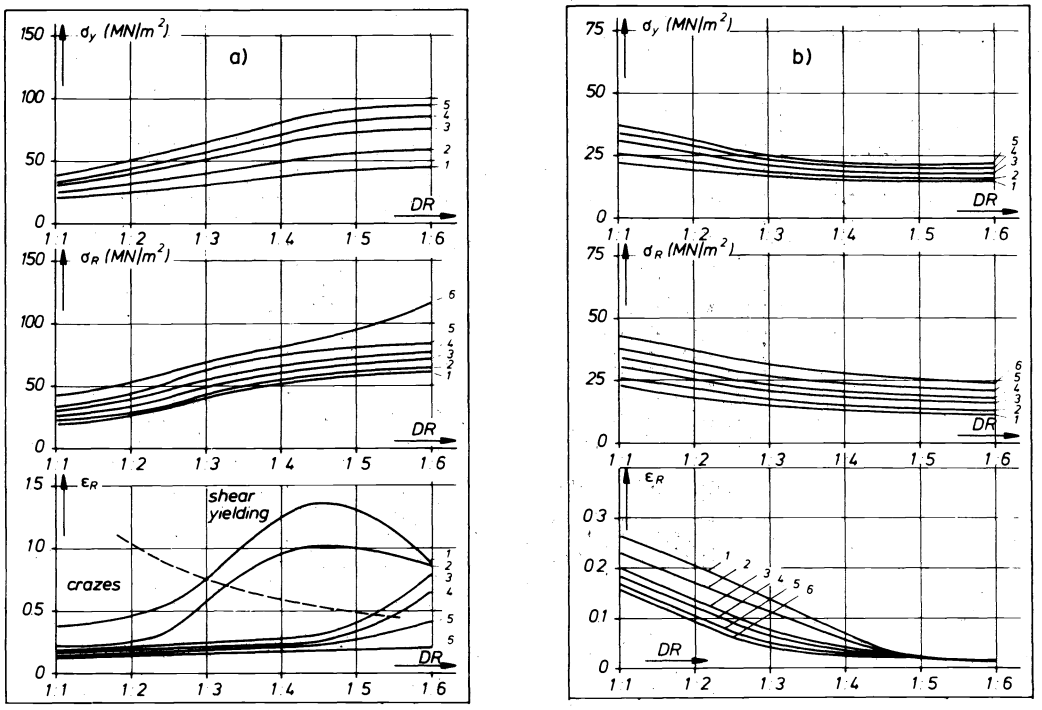

Fig. 23. Tensile behaviour of unoriented and oriented specimens of HIPS I. Specimens according to ISO/R 527, type 1, testing temperature 23 °C.
a) testing direction parallel to the direction of orientation
b) testing direction perpendicular to that direction
σ_y = yield stress, σ_R = rupture stress, ε_R = rupture strain
DR = draw ratio
tensile speeds $v_t \approx 7 \cdot \dot{\varepsilon}$
1) 8.33 10^{-5} cm/s 2) 8.33 10^{-3} cm/s 3) 8.33 10^{-1} cm/s
4) 8.33 cm/s 5) 83.3 cm/s 6) 833 cm/s

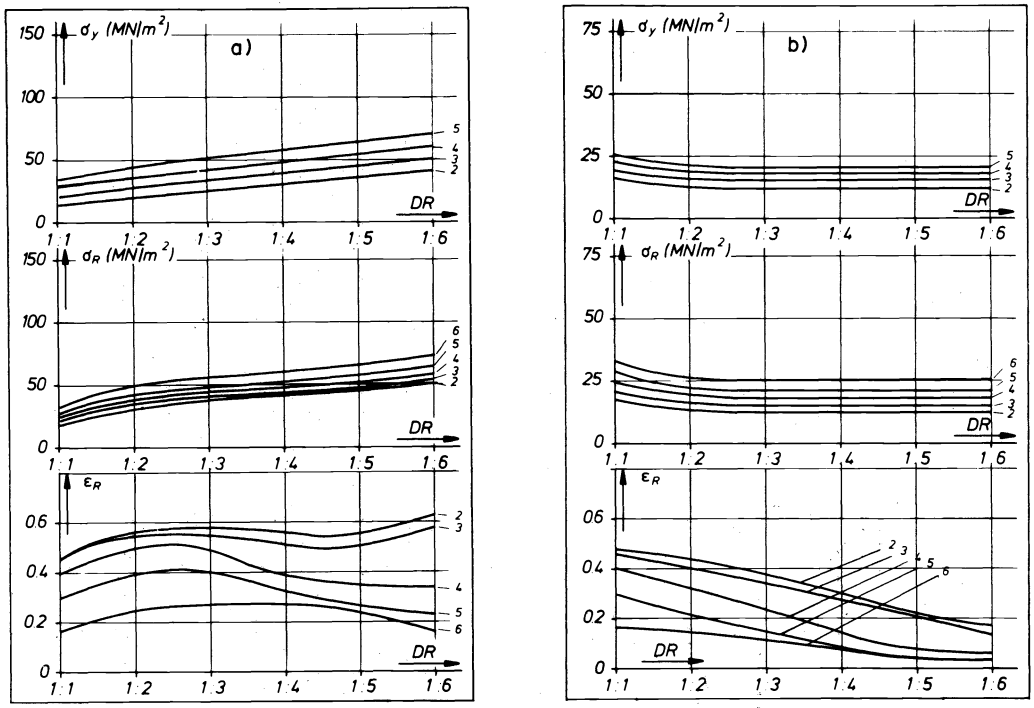

Fig. 24. Tensile behaviour of unoriented and oriented specimens of HIPS II. Tensile conditions and meaning of the symbols as in Fig. 23.

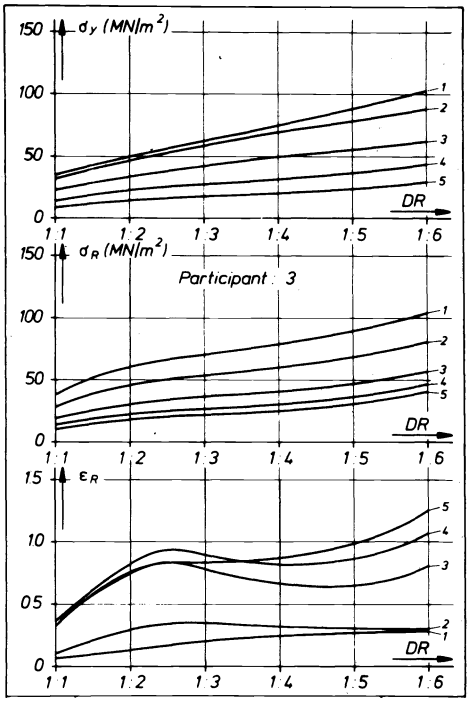

Fig. 25. Tensile behaviour of unoriented and oriented specimens of HIPS II. Specimens and meaning of the symbols as in Figs. 23 and 24; testing direction parallel to the direction of orientation, testing speed v_t = 8.33 10^{-1} cm/s, $\dot{\varepsilon} \approx 1.19\ 10^{-1}\ s^{-1}$, testing temperatures:
1) - 50 °C, 2) - 20 °C, 3) + 23 °C, 4) + 50 °C, 5) + 70 °C.

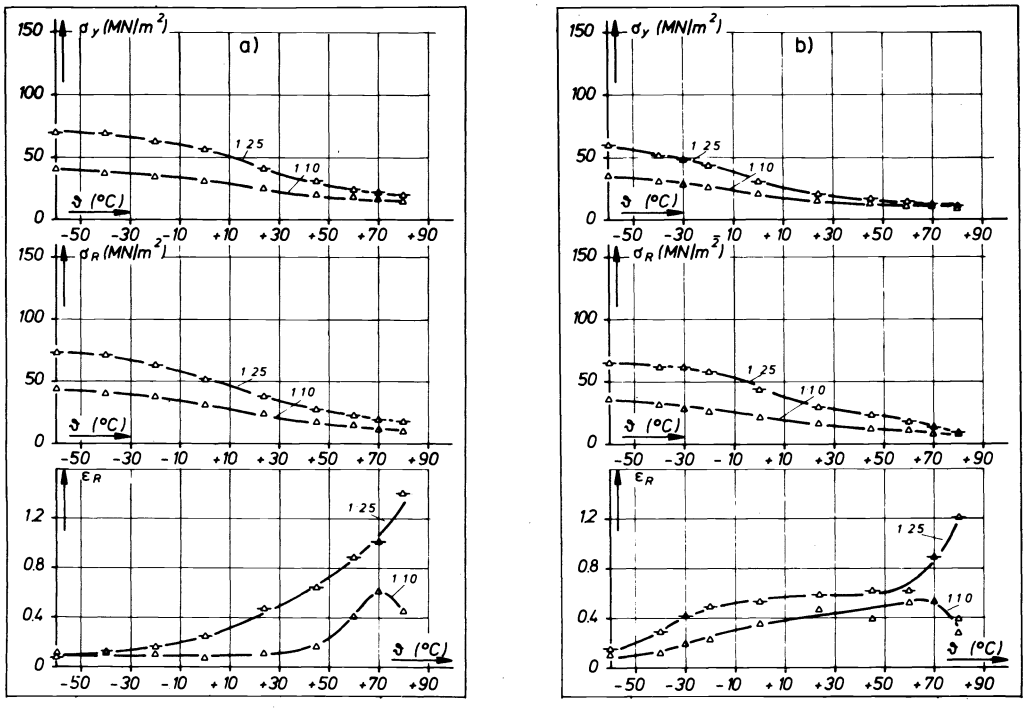

Fig. 26. Tensile behaviour of unoriented specimens and of specimens oriented by drawing up to DR = 1:2.5 of HIPS I (a) and II (b). Specimens and meaning of the symbols as in Figs. 23 to 25; testing direction parallel to the direction of orientation, testing speed v_t = 8.33 10^{-3} cm/s, $\dot{\varepsilon} \approx 1.19\ 10^{-3}\ s^{-1}$
ϑ = testing temperatures.

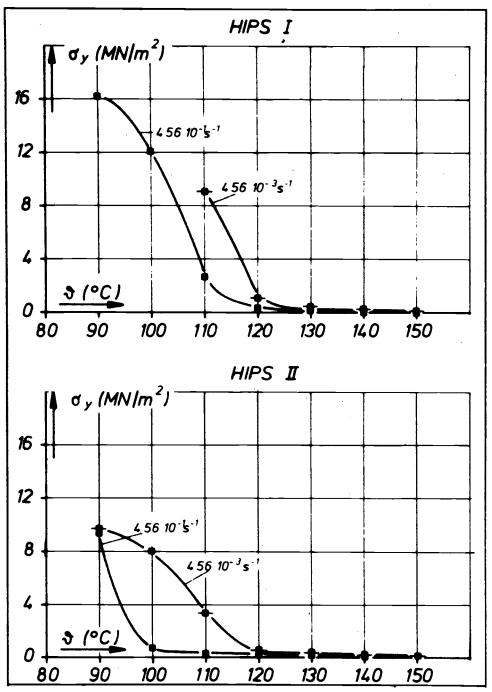

Fig. 27. Yield stress σ_y of unoriented specimens of HIPS I and II as a function of the testing temperature ϑ.

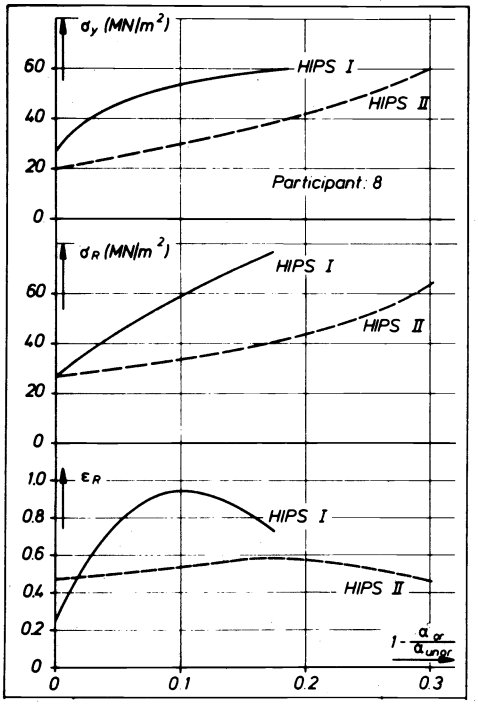

Fig. 28. Comparison of the tensile behaviour of HIPS I and II, showing dependence on the orientation measured with the aid of linear thermal expansion coefficient α.
Meaning of the symbols as in Fig. 23 to 26,
testing speed v_t = 8.33 10^{-3} cm/s, temperature 23 °C,
single values see Fig. 35.

conditions of both testing devices are very similar, their results can be compared with each other. As Fig. 30 shows, there is fairly good agreement between both laboratories. In contrast to its behaviour in the uniaxial impact test, HIPS II turned out to be the better material when tested with the aid of the multiaxial test. The force, the deformation, and the energy consumed at the point of first damage of HIPS II (oriented as well as unoriented) are somewhat higher than the corresponding values of HIPS I. All the quantities mentioned decrease for both materials with increasing orientation.

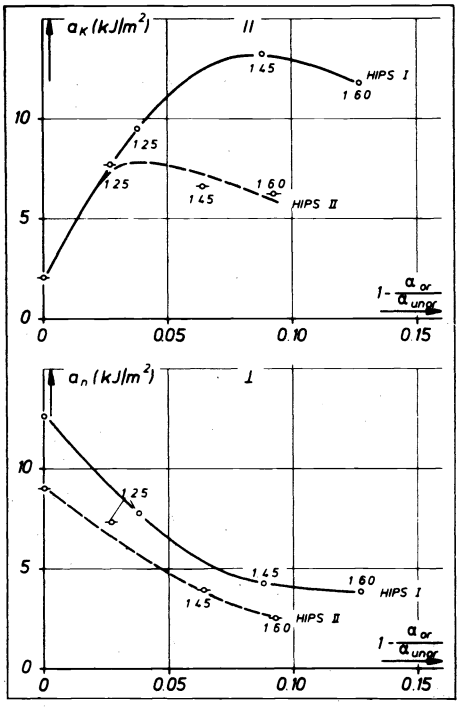

Fig. 29. Results of Charpy impact test on specimens of HIPS I and II (according to DIN 53 453).
a_k = impact resistance of notched specimens with the main axis parallel to the drawing direction
a_n = impact resistance on unnotched specimens with the main axis perpendicular to the drawing direction
DR = draw ratio
testing temperature 23 °C

6.3 CREEP PROPERTIES

Participants 1, 4, 5, and 7 performed creep measurements on the specimens of HIPS I and II delivered by participant 8 to all the participants. The participants mentioned measured the creep strain of the unoriented specimens loaded with 3 and 11 MN/m^2 whereas participants 1 and 7 also determined the creep compliances of the oriented specimens by applying stresses between 11.9 and 25 MN/m^2. The results of all these measurements are shown in Figs. 31 and 32. As is to be seen, the agreement between the individual laboratories is fairly good. Furthermore Fig. 32 shows that the creep compliance of HIPS I and II has already decreased considerably at a relatively slight orientation. Further orientation has only a small additional influence. Owing to the higher rubber phase volume of HIPS II the compliances of the unoriented as well as of the oriented specimens of this material exceed those of the HIPS I specimens. Furthermore the increase of the compliance of HIPS II, especially if this material is unoriented, is somewhat more pronounced with increasing time than that of the compliance of HIPS I.

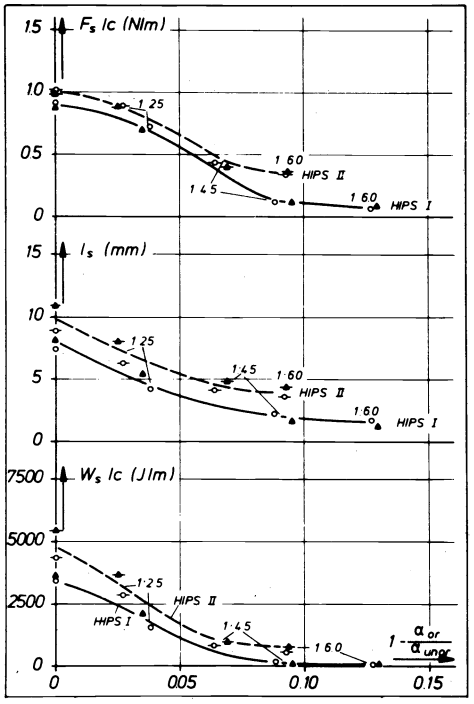

Fig. 30. Results of multiaxial impact tests on specimens of HIPS I and II (from both participants in principle according to DIN 53 443)
F_S = force at the first damaging of the specimen
l_S = deformation (measured in the direction of penetration) at the first damaging
W_S = energy consumed at the first damaging
c = thickness of the specimen
DR = draw ratio
testing temperature 23 °C

6.4 TIME- AND TEMPERATURE-DEPENDENT MODULI

As an example the Young's modulus of unoriented HIPS I is shown in Fig. 33a as a function of the logarithm of the time (from the beginning of the experiment in question). The modulus was calculated from bending vibration experiments of participants 1 and 8, from stress relaxation and tensile tests performed by participant 8, and from creep measurements carried out by participants 1, 4, 5, and 7. Although there is a rather great scattering of the results, the figure shows clearly the decrease of the modulus with increasing time that is to be expected for a viscoelastic polymer. Fig. 33b shows the dependence of Young's modulus (measured at 10 sec) of HIPS I and II on the draw ratio (specimens delivered by participant 8 to all the participants). Again HIPS II has the lower modulus because of the higher rubber phase volume of this material. Nevertheless the moduli of both materials increase almost identically with increasing draw ratio.

The temperature-dependent shear moduli of the oriented materials were determined by participant 1. His results were briefly condensed in section 2.4.

6.5 ENVIRONMENTAL STRESS CRACKING

The environmental stress cracking resistance of the unoriented as well as of the oriented materials was examined by participant 8 with the aid of the "Steel Ball Impression Method" according to DIN 53 449. Specimens with a length of 50 mm and a width of 6 mm were cut from the sheets perpendicular to the orientation direction. Circular holes with a diameter of 3 mm were drilled in the middle of the flat side of the specimens. Steel balls with a slightly oversized diameter were then pressed into the holes, the oversize being graduated within a set of specimens. Finally one half of the specimens

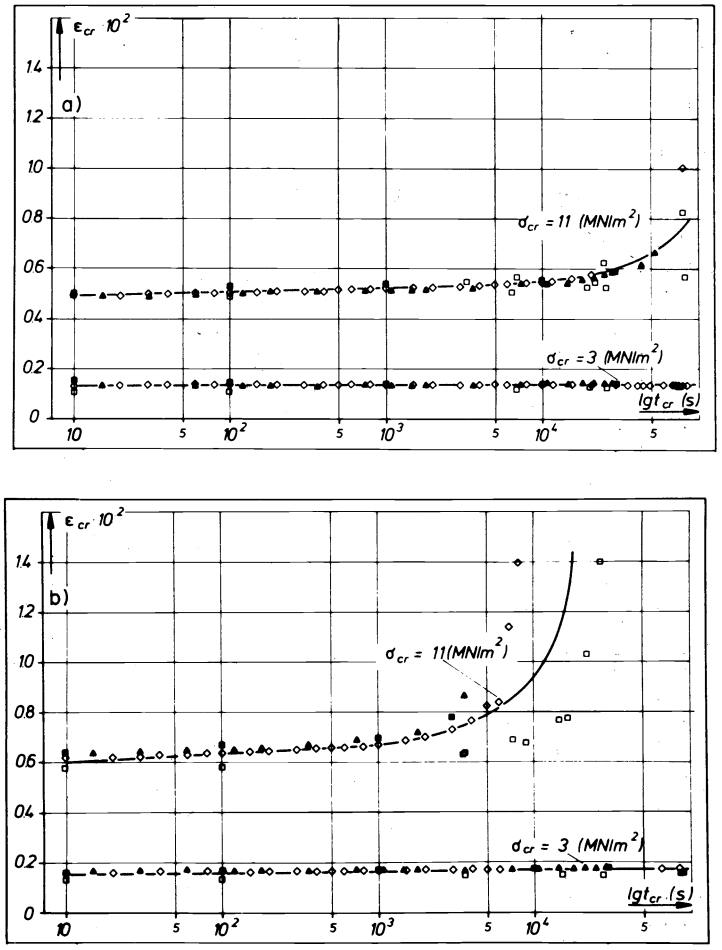

Fig. 31. Creep strain ε_{cr} of unoriented specimens of HIPS I (a) and II (b) as a function of the logarithm of the creep time t_{cr}; testing temperature 23 °C.

was put into ethanol for 60 minutes whereas the other half remained in air for 7 days. After this treatment the tensile strength of the specimens was measured at a tensile strain rate of 20 mm/min. The number of specimens examined this way was 5 per draw ratio and per ball oversize step. From the tensile strength of all specimens having the same draw ratio the ball oversize was determined at which the strength was 5 % less than that of a specimen with a hole but without a pressed-in ball (oversize zero). The ratio of these oversizes taken from alcohol- and from air-treatment specimens is defined as the "environmental stress cracking resistance" R_t of the material under test. R_t reaches the value one if the material is absolutely resistant to stress cracking. In Fig. 34 the measured R_t values of HIPS I and II are presented. Obviously HIPS I is considerably more sensitive to environmental stress cracking than HIPS II. Also, the decrease of the environmental stress cracking resistance with increasing draw ratio is more pronounced for HIPS I than for HIPS II.

7 DEPENDENCE OF THE MECHANICAL PROPERTIES ON THE ORIENTATION OF THE PS MATRIX AND ON THE DEFORMATION OF THE RUBBER PARTICLES

Previously it was found by participant 8 (see (7)) that for a number of oriented polymers there exist definite relationships between the molecular orientation and the mechanical properties, independently of the stretching conditions and of the draw ratio. Even if the orientation of stretched specimens was diminished by annealing at constant draw ratio (see 4.4) the mechanical properties followed the same relationships as are valid for stretching experiments.

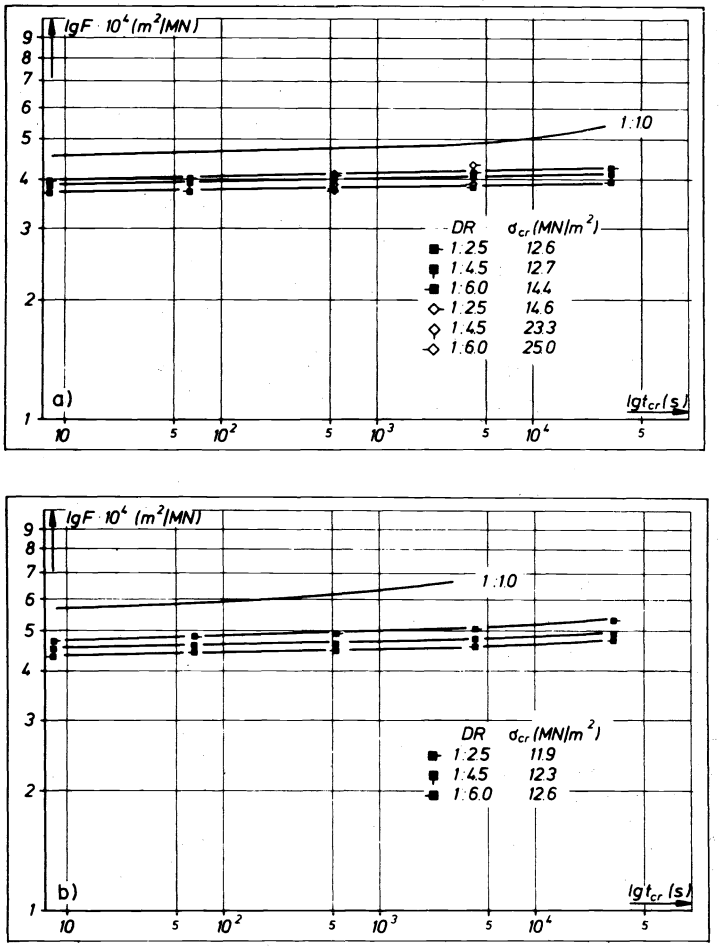

Fig. 32. Logarithm of the creep compliance F_{cr} of unoriented and oriented specimens of HIPS I (a) and II (b) as a function of the logarithm of the creep time t_{cr}; testing temperature 23 °C.

It was therefore of interest to check whether or not these findings are also true for rubber-modified polymers and, in addition, to investigate the influence of the deformation of the rubber particles on the mechanical properties in this case. For this reason the data obtained by tensile tests (performed with $\dot{\varepsilon} \approx 1.19\ 10^{-3}\ s^{-1}$) on all the specimens, i.e. of those additionally stretched (and partly annealed) as well as of those taken from the oriented sheets, were plotted in Fig. 35 as functions of the birefringence Δn and of the orientation function f_{or} calculated from the linear thermal expansion coefficient.

Despite of the statistical scatter of the points, figures 35a and b indicate the existence of definite relationships between the molecular orientation and the mechanical properties in this case too. Since only the orientation of the PS matrix is measured by Δn and f_{or}, and since very different axial ratios of the rubber particles are found at equal f_{or} values (see Fig. 36), it must be concluded, furthermore, that at a given orientation of the matrix the deformation of the rubber particles does not influence the mechanical properties of the system markedly.

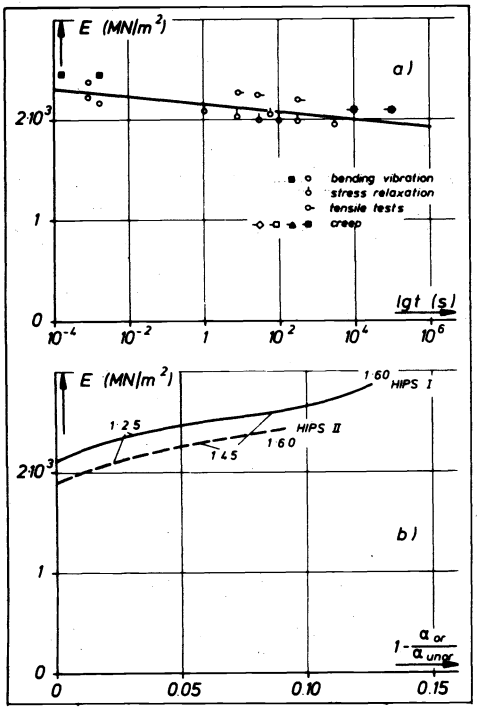

Fig. 33. a) Young's modulus E of unoriented HIPS I measured by several methods as a function of the logarithm of the time.
b) The dependence of the Young's moduli E of oriented HIPS I and II on the orientation ;
measuring temperature for a) and b) 23 °C.

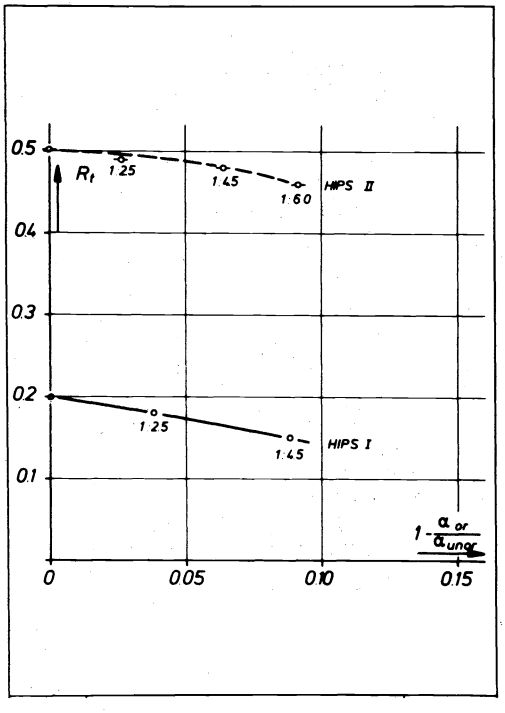

Fig. 34. Environmental stress cracking resistance R_t of HIPS I and II as a function of the orientation (as to the meaning of R_t see the text).

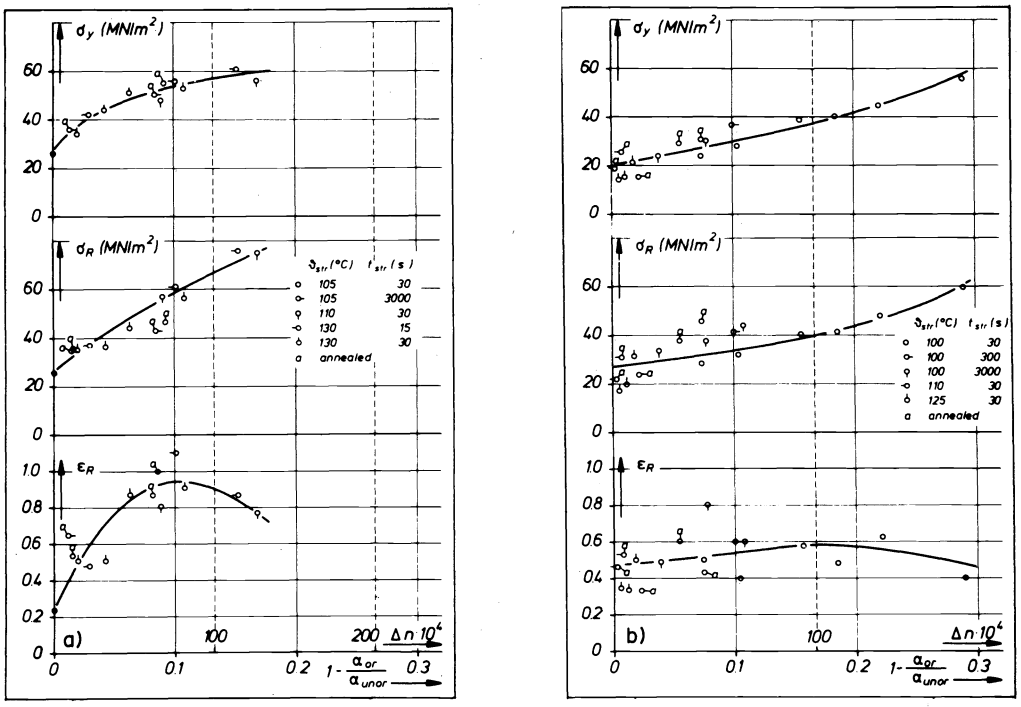

Fig. 35. The mechanical properties of HIPS I (a) and II (b) (obtained from tests performed with the tensile speed $v_t = 8.33\ 10^{-3}$ cm/s on the specimens distributed to all participants as well as on the specimens individually stretched by participant 8) as functions of the birefringence Δn and of the orientation function f_{or} calculated from the linear thermal expansion coefficient α.

Specimens strip-shaped, length between the clamps 70 mm; testing direction parallel to the direction of orientation; testing temperature 23 °C
σ_y = yield stress, σ_R = rupture stress, ε_R = rupture strain

8 CONCLUSIONS

From the results the following conclusions can be drawn:

- The molecular orientation of the PS matrix of rubber-modified polystyrene can be determined by measuring the optical birefringence Δn or by calculating Hermans' orientation function f_{or} from the linear thermal expansion coefficient α. Between Δn and f_{or} there exists a definite linear relationship, independent of the stretching conditions but dependent on the material in question. Under given stretching conditions (temperature and time or strain rate) the frozen-in stress and its entropic part and - with reservations - the length reversion ratio (shrinkage) can also be used for characterizing the orientation state of the matrix material.

- Owing to the molecular relaxation mechanisms of the matrix material the orientation of the molecules relaxes during the stretching process. If the specimens are stretched at sufficiently high temperatures with constant crosshead speed the generation and the relaxation of the orientation obeys the superposition principle, and, in addition, the generation of the orientation follows a linear relationship between the orientation and the strain. The theory of rubber elasticity can be applied to the oriented matrix material, provided that the stretching process was performed within a temperature range that is sufficiently far above Tg but below a value at which the chain molecules can no longer be treated as a Gaussian network.

- The deformation of the rubber particles embedded in the matrix material depends on the draw ratio and the stretching conditions. Only at low

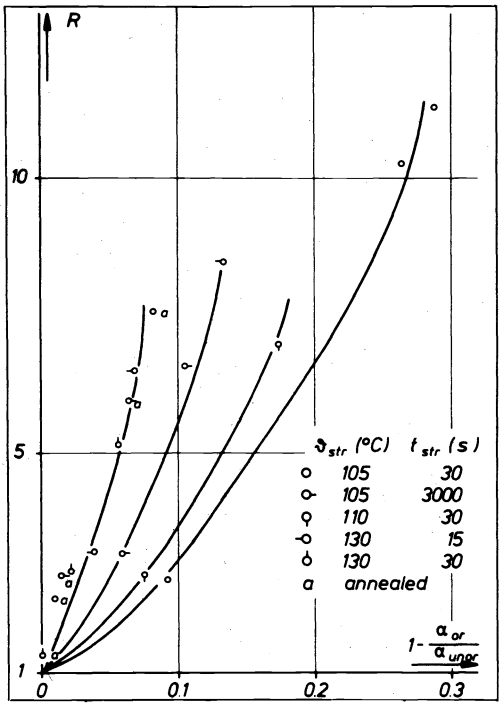

Fig. 36. Axial ratio R of the rubber particles in specimens of HIPS I stretched under various conditions (and partly annealed) as a function of the orientation of the PS matrix calculated from the linear thermal expansion coefficient α.

temperatures and short stretching times do the rubber particles deform in conformity to the matrix. Otherwise their deformation falls short more or less with respect to the matrix deformation.

- The mechanical strength and the extensibility of the rubber-modified system, measured parallel to the direction of orientation, are improved by orientation. The increase of the extensibility, which is unusual for polymers, is due to a transition from deformation by crazing to deformation by shear yielding. This transition does not depend on the rubber content but is characteristic of polystyrene (7,8).

- The two high impact polystyrenes (HIPS I and II) do not differ much from each other in their molecular weight or its distribution but more with regard to their glass transition temperatures Tg (unlike HIPS II, HIPS I contains no paraffin oil) and to their effective rubber phase volume (in the rubber particles of HIPS II more polystyrene is included). HIPS I (having the higher Tg and the lower rubber phase volume) can be oriented to a higher degree at a given temperature than HIPS II. Furthermore HIPS I is somewhat stronger, especially if it is oriented, and able to deform more easily by shear yielding in the oriented state. On the other hand HIPS II (having the higher rubber phase volume) tends more to forming crazes. Therefore, if it is not oriented, the extensibility of this material exceeds that of HIPS I considerably.

- As had formerly been found in the case of pure polystyrene, the mechanical properties of rubber-modified polystyrenes turned out to be definite functions of the molecular orientation of the matrix material, independent of the stretching conditions and, in this case, also of the deformation of the rubber particles.

The author is very much indebted to the other participants in the programme reported here for helpful cooperation and particularly to Dr. C.B. Bucknall, Cranfield Institute of Technology, for reviewing the English text.

REFERENCES

1. T. T. Jones, J. Pol. Sci. 16c, 3845 (1978)
2. A. Gonze, Pure. Appl. Chem. 18, 553 (1969)
3. J. L. S. Wales, Pure. Appl. Chem. (1968) and 20, 331 (1969)
4. H. Oberst a. W. Retting, J. Macromol. Sci. Phys. B5(3), 559 (1971)
5. A. Gonze a. J. Chauffoureaux, Pure. Appl. Chem. 35, 315 (1973)
6. J. Meissner, Pure. Appl. Chem. 42, 553 (1975)
7. W. Retting, Colloid a. Polymer Sci. 253, 852 (1975)
8. T. T. Jones, Pure. Appl. Chem. 45, 39 (1976)
9. J. Chauffoureaux, Pure. Appl. Chem. 47, 333 (1976)
10. A. J. de Vries, C. Bonnebat a. J. Beautemps: Uni- and biaxial orientation of polymer films and sheets, presented at 5th EPS conference on Macromol. Phys. Budapest, Apr. 1976, to be published in J. Pol. Sci. C
11. G. Cigna, J. Appl. Pol. Sci. 14, 1781 (1970)
12. G. Cigna, S. Matarrese, G. F. Biglione, J. Appl. Pol. Sci. 20, 2285 (1976)
13. H. Gerrens, Fortschr. Hochpol. Forschung 1, 234 (1959)
14. A. J. de Vries a. C. Bonnebat, Polymer Eng. a. Sci. 16, 93 (1976)
15. L. R. G. Treloar, Trans. Faraday Soc. 43, 277 (1947)
16. P. H. Hermans a. Pl Platzek, Kolloid Z. 88, 68 (1939)
17. J. Hennig, J. Pol. Sci. C. No. 16, 2751 (1967), Kunststoffe 57, 385 (1967)
18. L. R. G. Treloar: The Physics of Rubber Elasticity, Oxford University Press, London (1958)
19. J. F. Rudd a. E. F. Gurnee, J. Pol. Sci. A1, 2857 (1963)
20. J. D. Ferry: Viscoelastic Properties of Polymers, J. Wiley & Sons, Inc., New York, London (1970)
21. W. Retting, to be published
22. E. Underwood, Amer. Soc. Metals a. Quart. 11, 62 (1962)
23. T. Casiraghi, G. Castiglioni, Materie Plastische e. Elastomeri 42 (10), 765 (1976)
24. H.-P. Gilfrich et al. Kunststoffe 63, 327 (1973)